ผลของการเติมเฮกเซนที่มีต่อการเผาไหม้พาทาลิกแอนไฮไดรด์บนตัวเร่งปฏิกิริยา V_2O_5/TiO_2 ที่ได้รับการเคลือบผิวด้วยออกไซด์โลหะทรานซิชันและแมกนีเซียมออกไซด์

นายสุรกิจ ปัญจสมุทร

วิทยานิพนธ์นี้เป็นส่วนหนึ่งของการศึกษาตามหลักสูตรปริญญาวิศวกรรมศาสตรมหาบัณฑิต
สาขาวิชาวิศวกรรมเคมี ภาควิชาวิศวกรรมเคมี
คณะวิศวกรรมศาสตร์ จุฬาลงกรณ์มหาวิทยาลัย
ปีการศึกษา 2546

ISBN 974-17-5050-1

EFFECTS OF HEXANE ADDITION ON PHTHALIC ANHYDRIDE COMBUSTION OVER V_2O_5/TiO_2 CATALYSTS IMPREGNATED WITH TRANSITION METAL AND MAGNESIUM OXIDE

Mr. Surakit Punjasamud

A Thesis Submitted in Partial Fulfillment of the Requirements
For the Degree of Master of Engineering in Chemical Engineering
Department of Chemical Engineering
Faculty of Engineering
Chulalongkorn University
Academic Year 2003

ISBN 974-17-5050-1

Thesis Title	EFFECTS OF HEXANE ADDITION ON PHTHALIC ANHYDRIDE COMBUSTION OVER V_2O_5/TiO_2 CATALYSTS IMPREGNATED WITH TRANSITION METAL AND MAGNESIUM OXIDE
By	Mr. Surakit Punjasamud
Field of Study	Chemical Engineering
Thesis Advisor	Associate Professor Tharathon Mongkhonsi, Ph.D.

Accepted by the Faculty of Engineering, Chulalongkorn University in Partial Fulfillment of the Requirements for the Master's Degree

……..Dean of the Faculty of Engineering
(Professor Direk La vansiri, Ph.D.)

THESIS COMMITTEE

……..Chairman
(Associate Professor Suttichai Assabumrungrat, Ph.D.)

……..Thesis Advisor
(Associate Professor Tharathon Mongkhonsi, Ph.D.)

……..Member
(Artiwan Chotipruk, Ph.D.)

……..Member
(Joongjai Panpranot, Ph.D.)

สุรกิจ ปัญจสมุทร : ผลของการเติมเฮกเซนที่มีต่อการเผาไหม้พาทาลิกแอนไฮไดรด์บนตัวเร่งปฏิกิริยา V_2O_5/TiO_2 ที่ได้รับการเคลือบผิวด้วยออกไซด์โลหะทรานซิชันและแมกนีเซียมออกไซด์ (EFFECTS OF HEXANE ADDITION ON PHTHALIC ANHYDRIDE COMBUSTION OVER V_2O_5/TiO_2 CATALYSTS IMPREGNATED WITH TRANSITION METAL AND MAGNESIUM OXIDE)

อ. ที่ปรึกษา : รศ. ดร. ธราธร มงคลศรี, 107 หน้า. ISBN 974-17-5050-1

ทำการศึกษาผลของการเติมเฮกเซนในปฏิกิริยาการเผาไหม้ของสารประกอบพาทาลิกแอนไฮไดรด์บนตัวเร่งปฏิกิริยาวานาเดียมออกไซด์บนตัวรองรับไททาเนีย ที่ได้รับการเสริมด้วยโลหะทรานซิชัน (เหล็ก ทองแดง สังกะสี และ โมลิบดีนัม) และแมกนีเซียมออกไซด์ ผลการทดลองแสดงให้เห็นว่า การเติมเฮกเซนทำให้เกิดการแข่งขันกับพาทาลิกแอนไฮไดรด์ในการเกิดปฏิกิริยาทำให้เกิดการยับยั้งในปฏิกิริยาที่ว่องไวน้อยกว่า โดยขึ้นกับ(ความเหมาะสม)ชนิดของตัวเร่งปฏิกิริยาแต่ละชนิดกับสารตั้งต้นดังที่พบในตังเร่งปฏิกิริยาทองแดง สังกะสี โมลิบดีนัม และยังพบว่าเกิดการสนับสนุนการเผาไหม้ของพาทาลิกแอนไฮไดรด์และเฮกเซนบนตัวเร่งปฏิกิริยาที่ได้รับการเสริมด้วยเหล็ก และแมกนีเซียมออกไซด์ ซึ่งน่าจะมีผลจากการเกิดปฏิกิริยาออกซิเดชันบางส่วนของสารตั้งต้นเกิดเป็นสารมัธยันต์ซึ่งส่งเสริมการเผาไหม้ของทั้งสองปฏิกิริยา

ภาควิชา……**วิศวกรรมเคมี**…….. **ลายมือชื่อนิสิต**……..

สาขาวิชา……**วิศวกรรมเคมี**……. **ลายมือชื่ออาจารย์ที่ปรึกษา**……

ปีการศึกษา……2546……

#4570615021: MAJOR CHEMICAL ENGINEERING
KEY WORD: COMBUSTION / TRANSITION METAL OXIDE CATALYSTS / PHTHALIC ANHYDRIDE / HEXANE

SURAKIT PUNJASAMUD: EFFECTS OF HEXANE ADDITION ON PHTHALIC ANHYDRIDE COMBUSTION OVER V_2O_5/TiO_2 CATALYSTS IMPREGNATED WITH TRANSITION METAL AND MAGNESIUM OXIDE
THESIS ADVISOR: ASSOC.PROF. THARATHON MONGKHONSI, Ph.D.
107 pp. ISBN 974-17-5050-1.

The effect of hexane addition on the combustion of phthalic anhydride over V_2O_5/TiO_2 catalysts promoted with transition metal (Cu, Fe, Mo or Zn) and magnesium oxide was investigated. The results showed that there were competitive adsorption of phthalic anhydride and hexane on the catalyst. For Cu, Mo and Zn, catalysts phthalic anhydride and hexane competitively adsorbed and reacted on same active sites. Therefore, the combustion of phthalic anhydride or hexane hindranced each other depended on the adsorption ability on each catalyst. The Fe catalyst showed different result i.e. the combustions of the phthalic anhydride and hexane was promoted when both reactants were fuel together.

Department ...…Chemical Engineering….. Student's signature ……
Field of study… Chemical Engineering … Advisor's signature …….
Academic year……2003.…….

ACKNOWLEDGEMENTS

The author would like to express his greatest gratitude and appreciation to his advisor, Associate Professor Tharathon Mongkhonsi for his invaluable guidance, providing value suggestions and his kind supervision throughout this study. In addition, he is also grateful to Associate Professor Suttichai Assabumrungrat, as the chairman, Dr. Joongjai Panpranot and Dr. Artiwan Chotipruk, who have been member of thesis committee.

Many thanks for kind suggestions and useful help to Miss Pimporn Chaicharus, Miss Nalinpan Charoenruay, Miss Sujaree Kaewgun, Miss Kanda Pattamakomsan, Miss Chitlada Sakdamnuson, Miss Tananya Vongthavorn, Mr. Natthaya Kiattisirikul, Mr. Jitkarun Phongpatthanapanich, Mr. Somyod Sombatchaisak and many friends in the petrochemical laboratory who always provide the encouragement and co-operate along the thesis study.

Finally, he would like to dedicate the achievement of this work to his parents, who have always been the source of his support and encouragement.

CONTENTS

CONTENTS (Cont.)

LIST OF TABLES

TABLES **PAGE**

LIST OF FIGURES

FIGURES **PAGE**

CHAPTER I

INTRODUCTION

The problem of air pollution abatement from waste gases is a topic of growing concern in relation to the complete oxidation of volatile organic compounds (VOCs) and carbon monoxide. The main processes currently used are thermal and catalytic incinerations. In both processes the organic compounds are completely oxidized by oxygen to carbon dioxide and water. The effluent gas from phthalic anhydride manufacturing was the one of air pollution which we concern.

Phthalic anhydride is an important organic chemical used mainly in the preparation of plasticizers for PVC. The first process was based on the liquid-phase oxidation of naphthalene. However, it was the development of the gas–phase air oxidation process of o-xylene. Among the various catalysts used for the oxidation of *o*-xylene those containing V_2O_5 supported on titania (TiO_2) show the best performance [Dias (1995)].

The aromatic reactant was vapourised and mixed with air in gaseous phase. The concentration of the aromatic was limited by the lower explosive limit of the gas mixture. The gas mixture then flowed to a reactor containing several thousands of catalyst tubes. The products formed, the anhydrides, were recovered by cooling the product gas stream using a condenser.

At the condenser, it was known that the lower coolant temperature, the higher product recovery. In practice, the temperature at the condenser was limited by the concentration of water in the product gas stream. If water was allowed to condense, corrosion will occur. The effluent gas leaving the condenser, therefore, still contained traces of organic compounds including the hydrocarbon reactant and the anhydride product. The large amount phthalic anhydride have experienced irritation of the eyes, the skin, and the respiratory system. It can also cause lung sensitization.

Because of these reason liminating the remaining organic compounds from the effluent gas was necessary. At present, the removal could be carried out by sending the effluent gas which still contained high oxygen concentration to a furnace. This method, however, may cause problem concerning the energy balance of the plant and NO_x forming from high temperature combustion. Catalytic combustion was an alternative for controlling volatile organic compounds (VOCs) emissions. It is a well-known technology that is being used in a variety of industrial applications. In this process, very high destructive efficiencies can be achieved at relatively low operating temperatures resulting in considerable environmental and economic benefits in comparison to the case of the more conventional thermal combustion.

There were two catalyst families that could completely oxidize organic compounds. One was the Pt-based catalysts and the other one was the acidic metal oxide based catalysts.

The Pt-based catalysts could initiate the combustion of the organic compounds at a lower temperature than the acidic metal oxide-based catalysts, typically 100-200°C lower. But the Pt-based catalysts could not withstand prolong operation in a high oxygen concentration atmosphere. The acidic metal oxide-based catalysts worked better in the latter case.

An important nature of the acidic metal oxide catalyst is its capability to adsorbed acidic organic compounds. On the acidic surface, the acidic organic compounds are less likely to be adsorbed. The further oxidation of the acidic compound to combustion products, therefore, is low. Because of this reason, the acidic metal oxide catalyst becomes a selective oxidation catalyst for the production of anhydrides because it has low ability to further oxidise the anhydride products formed. On the contrary, this behavior causes problem when one has to use it as a combustion catalyst.

In order to overcome the aforementioned problem, it was proposed to dope a MgO to an acidic metal oxide catalyst to enhance the adsorption of the acidic organic compounds. It has been shown that magnesium oxide promoted the adsorption of

phthalic anhydride leading to better combustion of the phthalic anhydride for the acidic and amphoteric transition metal oxides [Tongsang (2001) and Umpo (2001)]. Next research has aimed to study the possibility to improved the spent V_2O_5 catalysts, normally removed after deactivated, for used as catalysts in combustion of phthalic anhydride. The spent cat is simulated by prepared the V_2O_5 /TiO_2 catalyst which has the same composition as the catalyst for production of phthalic anhydride. Then promoted with transition metal and magnesium oxide were used as catalysts for the combustion of phthalic anhydride [Charoenruay (2003)].

The present work is a cocurrent research with work of Charoenruay (2003). This work studied the possibility to use hydrocarbon to enhance catalytic combustion activity of phthalic anhydride V-Mg-O/TiO_2 catalyst with different transition metals (Zn, Cu, Mo and Fe) loading. In the real phthalic anhydride process, the concentration of phthalic anhydride in the effluent gas and the gas temperature are so low that the combustion reaction can not self initiate and maintain without the supply of external heat. The present work focused on how to maintain the combustion reaction after the effluent gas was heated up to a temperature which could initiate the combustion reaction. The idea of this research came from the fact the combustion of organic compounds is an exothermic reaction which generates energy. If another reactant which could be completely oxidized by the catalysts being investigated was co-feed with phthalic anhydride, the heat generated from the combustion of the added reactant could make the overall combustion reaction self maintain. The choice of the second reactant is important. It should be cheap, easily available, reacts easily and completely, yields high energy and should not interfere with the phthalic anhydride combustion reaction. However, there is no reactant meeting all the above conditions. In the research, saturated hydrocarbon, was selected because of its price, availability and heat of combustion, though its reactivity was still not in doubt. Hexane was used as a representative of saturated hydrocarbon.

In this study the V-Mg-O/TiO_2 catalyst with different transition metal (Zn, Cu, Mo and Fe) loading had been used to investigate the combustion for phthalic anhydride in presence of hexane.

This present work is organized as follows:

Chapter II contains literature reviews of phthalic anhydride processes, transition metal oxides, supported transition metal oxide catalysts on various reactions and effects of mixture on nonoxidation catalyst reaction.

The theory of this research, studies about the oxidation reaction and its possible mechanisms, the reaction of anhydrides, and the properties of transition metal oxides are presented in chapter III.

Description of experimental systems and the operational procedures are described in chapter IV.

Chapter V reveals the experimental results of the characterization of Fe-V-Mg-O/TiO_2, Zn-V-Mg-O/TiO_2, Mo-V-Mg-O/TiO_2 and Cu-V-Mg-O/TiO_2 catalysts and the oxidation reaction of phthalic anhydride over these catalysts.

Chapter VI contains the overall conclusion emerged from this research.

Finally, the sample of calculation of catalyst preparation, external and internal diffusion limitations, calibration curves from area to mole of phthalic anhydride, hexane and carbon dioxide, and data of the experiments which had emerged from this study are included in appendices at the end of this thesis.

CHAPTER II

LITERATURE REVIEW

The heterogeneous catalytic oxidation of organic compounds was an important and intensely studied area. However, most reported research deals with the partial oxidation of petrochemical feedstocks to make products of economic value, automotive exhaust catalysts, or CO oxidation. But this review focused on application to control of VOC by complete catalytic oxidation. The complete catalytic oxidation was widely used method for elimination of organic pollutants in gaseous streams to CO_2 and water.

The extant literature on the complete catalytic oxidation of hydrocarbon and substituted hydrocarbon has been written from two basic perspectives, in-depth laboratory investigations of pure components and more qualitative or investigations of very complex and ill-characterized mixtures. The laboratory involves a wide range of reactant concentration, temperature, pressure and reaction condition. The investigation of real mixtures also involves a similarly wide range of condition because the usual application is for end-of-pipe air pollution or odor control from various industrial sources. However, unlike most laboratory research, many studies of real mixture reported only overall gross performance and were not helpful in understanding the fundamental processes involved.

This chapter reviews the works about the combustion of phthalic anhydride on Cr, Mn, Fe, Ni, Cu, Zn, Mo and W promoted MgO on Al_2O_3 supported catalysts and V-Mg-O/TiO_2, the deactivation of an industrial V_2O_5/TiO_2 catalyst for oxidation of o-xylene into phthalic anhydride, the transition metal oxide, supported transition metal oxide catalysts in the various reactions, the catalytic combustion of other VOC, infrared studies of the reactive adsorption of organic molecules over metal oxides and catalytic combustion of VOC in mixtures.

2.1 Literature reviews

Toyada and Teraji (1980) invented a process that allows the treatment of byproducts obtained in the preparation of phthalic anhydride without creating secondary pollution. The byproducts may be low boiling point and/or high boiling point fractions obtained in the purification step by distillation of crude phthalic anhydride produced by the partial oxidation of o-xylene or naphthalene. Byproducts were treated by heating the byproducts to a temperature sufficient to maintain the byproducts in a molten state and thereafter atomizing air having a temperature of at 60°C for combustion. The byproducts may be low boiling point and/or high boiling point fractions obtained in the purification step by distillation of crude phthalic anhydride produced by the partial oxidation of o-xylene or naphthalene.

Keuneche *et al.* (1981) invented a process for continuously separating phthalic anhydride from the reaction gases of the catalytic oxidation of o-xylene and/or naphthalene by treating reaction gas mixture with a maleic anhydride absorbent. Absorption could be performed in two or more stages, preferably in two stages. The reaction gas, with a temperature from 135 - 150°C, was introduced into the absorption zone, and withdrawn at a temperature from 45 - 80°C from the absorption zone. The maleic anhydride, which was loaded with phthalic anhydride, was separated through distillation into raw phthalic anhydride as a bottoms product and an overhead product primarily containing maleic anhydride. The overhead product was then returned into the absorption zone. The raw phthalic anhydride was treated and then purified through distillation, e.g. in a continuous, two stage distillation in which light, volatile impurities, such as residual maleic anhydride and benzoic acid, were distilled off in the first stage and the pure phthalic anhydride was distilled in the second as an overhead product. The gas leaving the absorption zone and containing small amounts of maleic anhydride was scrubbed with water. The maleic acid solution recovered from this scrubbing was evaporated, the maleic acid was dehydrated and distilled, and a part of the maleic anhydride distillate was returned into the absorption zone.

Way and Peter (1981) invented an apparatus for recovery of vaporized phthalic anhydride from the gas streams. Phthalic anhydride was recovered from

gases in a multiple heat-pipe exchanger system, one or more for condensing phthalic anhydride from gases containing vapors thereof and one or more simultaneously melting out the condensed phthalic anhydride solids. The exchangers being switched in alternate cycles to melt out from the surfaces of the exchanger tube ends on which the phthalic anhydride solids were first accumulated, and to condense phthalic anhydride solids in the exchanger from which melting out cleared the phthalic anhydride. The cooling to recover phthalic anhydride was carried out with ambient air, and the heating to melt out accumulated phthalic anhydride was performed with hot gases.

Spivey (1987) reviewed the complete catalytic oxidation of volatile organics. The paper reviewed that both metal oxides and supported noble metals were active for many deep oxidations. Metal oxide catalysts were generally less active than were supported noble metals, but the were more resistant to poisoning. This poison resistance was suggested to be due to the high active surface area of metal oxides compared to supported noble metals. The most active single metal oxide catalysts for complete oxidation for a variety of oxidation reactions were usually found to be oxides of V, Cr, Mn, Fe, Co, Ni and Cu. The mechanism of oxidation on these oxide catalysts was generally thought to involve strong adsorption of the organic compound at an anionic oxygen site in the oxide lattice leading to the formation of an activated complex. This complex could then react further to yield products of complete combustion.

Gangwal *et al.* (1987) studied complete low-temperature deep oxidation of n-hexane and benzene over a 0.1% Pt, 3% Ni/γ-Al_2O_3 catalyst. These VOCs were subjected to oxidation as single components and as a binary mixture at temperatures ranging from 160 to 360°C. They found that n-hexane oxidation was significantly inhibited in the mixtures. An approach based on the Mars-Van Krevelen rate model was used to explain the results. Kinetic parameters were developed for the individual VOCs based on single component differential reactor data. These kinetic parameters were then incorporated into a proposed multicomponent Mars-Van Krevelen rate model to predict the experimental conversions in the binary mixture. The model was

found to be reasonably successful in predicting the conversion of benzene and n-hexane in their binary mixture.

Hess *et al.* (1993) studied catalysts containing metal oxides for use in the degenerative oxidation of organic compounds presented in exhaust gases from combustion plants. Metal oxide containing catalysts, which contained oxides of titanium and/or zirconium, oxides of vanadium and/or niobium, and oxides of molybdenum, tungsten, and chromium were investigated. It was found that the adding of alkaline earth metal sulfates produced a catalyst, which was clearly superior to catalysts composed only of the metal oxides. They found that the preferred catalyst should contain the following components: titanium dioxide, especially in the form of anatase, vanadium oxide in the form of V_2O_5 and tungsten oxide in the form of WO_3.

Kang and Wan (1994) studied the effects of acid or base additives on the catalytic combustion activity of chromium and cobalt oxides. It was found that the base additive could enhance the catalytic activity of Cr, Co oxides for carbon monoxide oxidation, but the acid additive reduced the activity. For ethane combustion, the addition of a base additive to the catalysts could reduce the ethane conversion. The selectivity of carbon dioxide, however, was increased to 100% because the rate of carbon monoxide oxidation was enhanced. On the other hand, the addition of acid additive to the catalyst gave an increase in ethane conversion, but the selectivity to carbon dioxide was reduced.

Busca *et al.* (1997) studied the transition metal mixed oxides as combustion catalysts. The catalysts have been tested in the catalytic combustion of methane, CO and H_2 (perovskites), of propane and of phenantrene. FT-IR experiments allowed to obtain a quite complete picture of the mechanism of catalytic combustion of C_3 organic compounds on spinel-type oxides $MgCr_2O_4$ and CO_3O_4. Nucleophilic oxygen species (lattice oxygen) is thought to be involved in both partial and total oxidation.

Larsson *et al.* (1997) investigated supported metal oxides for catalytic combustion of CO and VOCs. TiO_2 (anatase), SiO_2 and γ-$A1_20_3$ were used as supports for Co-, Cu-, Fe- and Mn-oxide with a loading of active phase corresponding to one theoretical layer. The catalysts were tested for the combustion of CO and toluene, and

the best combinations with active phase and support they found were submitted to a deactivation test in a waste gas incinerator for 50 days. The catalyst screening showed that CuO_x/TiO_2 was the most promising system. To design a catalyst with good activity and transport properties, they proposed to coated a macroporous substrate with TiO_2 for use as a support for Cu-oxide. Titania overlayers were prepared by precipitation from oxychloride, tetrachloride and alkoxide, and stabilisation with ZrO_2 and SiO_2 was tried. The results showed that precipitation from oxychloride gives the best properties and that addition of ZrO_2 gives enhanced activity to the catalyst, while SiO_2 addition produces increased stability.

Ozkan *et al.* (1997) investigated the partial oxidation of C_5 hydrocarbons over unpromoted and alkali-promoted V_20_5 catalysts. Products of this mild oxidation reaction include both maleic and phthalic anhydride. The apparent effect of alkali promotion was to facilitate the loss of surface oxygen species which were important in the activation of alkanes and the complete oxidation of intermediate species. Studies performed using 1-pentene as feed have indicated that once the first oxidative dehydrogenation step is eliminated, pentene oxidation proceeds readily towards maleic and phthalic anhydride formation.

Leklertsunthon (1998) investigated the oxidation property of a series of V-Mg-O/TiO_2 catalyst in the oxidation reaction of propane, propene, 1-propanol and carbon monoxide. It had been found that the catalytic behavior of the catalyst depended on the reactants. Propene and CO_2 were the major products in the propane oxidation reaction. The vanadium and magnesium contents affected the catalytic property of the V-Mg-O/TiO_2 catalyst in the reaction. The sequence of magnesium loading also affected the structure and catalytic performance of this catalyst. In addition, this catalyst was inactive for propene oxidation, from which it could be indicated that propene formed in propane oxidation reaction was not further oxidized to CO_2. According to 1-propanol oxidation, propionaldehyde was the main observable product at low reaction temperatures, and it was oxidized rapidly to CO_2 when the reaction temperature was increased. Moreover, the dehydration of 1-propanol became significant at high temperatures. It was found that the sequence of magnesium loading and magnesium content had no effect on the catalytic performance of the catalyst. On the other hand, increasing vanadium content improved the propene

selectivity and decreased the CO_2 selectivity. Finally, in CO oxidation, this catalyst was rather inactive. Since CO was an unobservable product in propane, propene and 1-propanol reactions, on the V-Mg-O/TiO_2 catalysts, CO was not produced in these three reactions.

Mongkhonsi and Kershenbaum (1998) studied the effect of deactivation of a V_2O_5/TiO_2 (anatase) industrial catalyst on reactor behavior during the partial oxidation of o-xylene to phthalic anhydride. Elemental C-H-N analysis of the results for catalyst pellets aged under a variety of operating conditions showed that some carbonaceous materials could deposit on the catalyst surface at most high reaction temperature, especially at high hydrocarbon concentration. The XRD and XPS results did not reveal the presence of vanadium oxides of V valency < 5+. The presence of carbon on the used catalyst pellet and the absence of any low oxidation state of vanadium from the XRD and XPS analyses indicated that the deposition of some carbonaceous materials was likely to be a major cause of catalyst deactivation when it was used in regions high hydrocarbon concentration. This deposited carbon compounds may slow down the reaction rate by a fouling process which reduced the effective activity surface area of the catalyst for further hydrocarbon adsorption. To effectively removed all the adsorbed compounds, the catalyst required reaction in an air stream at a temperature not less than 400°C over several hours, depending upon the past history of the catalyst.

Amiridis *et al*. (1999) studied the effect of metal oxide additives on the activity of V_2O_5/TiO_2 catalysts for the selective catalytic reduction of nitric oxide by ammonia. The results showed the presence of the second metal oxide phase had different effects on the SCR activity of the V_2O_5/TiO_2 catalyst depending on the nature of the additive. They observed that MoO_3, WO_3 and Nb_2O_5 additive promoted the SCR activity, while GeO_2, FeO_3 and CeO_2 had no significant effect on it, and MnO_2, Ge_2O_3, La_2O_3, SnO_2 and ZnO appeared to poison it. The results of this effort indicated that the presence of the additive metal oxides may affect a variety of catalyst properties, including the structure and reducibility of vanadia, and the overall amount and type of surface acidity. Among these factors the only one that correlated with SCR reactivity was the amount of surface Brönsted acid sites on the catalyst surface results in an increase in the SCR rate.

Brink *et al.* (1999) studied the catalytic combustion of chlorobenzene on a 2% Pt/γ-Al_2O_3 catalyst. Considerable amounts of polychlorinated benzenes were formed as by-products. They noted that the co-feeding of heptane practically eliminates this unwanted side-reaction. Moreover, the conversion of chlorobenzene occurs at much lower temperatures (the temperature at which 50% conversion drops from 305 to 225°C). Simultaneously, the conversion of heptane was retarded. The additions of other hydrocarbons had a similar effect. Water and heat produced by the combustion of the added hydrocarbon could not explain the increase in the destruction rate of chlorobenzene. Removal of Cl from the surface by the alkane appears to be the ruling factor.

Lietti *et al.* (1999) studied the characterization and reactivity of V_2O_5-MoO_3/TiO_2 de-NO_x SCR catalysts. The results showed that the V_2O_5-MoO_3/TiO_2 catalysts were very active in the reduction of NO by NH_3, and exhibited a higher reactivity with respect to the corresponding binary V_2O_5/TiO_2 and MoO_3/TiO_2 samples having the same V and Mo loading. The addition of Mo and V caused the formation of Brönsted sites and of stronger Lewis acid sites, if compared to TiO_2.

O'Malley and Hodnett (1999) studied the reactivity of a range of volatile organic compounds with differing functional groups over platinum catalysts supported on β-zeolite, mordenite, silica or alumina. Alcohols, ketones, carboxylic acids, aromatics and alkanes were used in the study. The reactivity pattern observed by them was alcohols > aromatics > ketones > carboxylic acids > alkanes, although some overlap was observed in that the more reactive alkanes were more readily oxidized than the less reactive carboxylic acids. The same order of reactivity was observed for all the catalysts studied here. A kinetic isotope effect was observed when deuterated acetone was compared to normal acetone, consistent with C–H bond cleavage being the slow step in the catalytic oxidation of this substrate. A correlation was found between the reactivity of the individual substrates and the strength of the weakest C–H bond in the structure. A single weak C–H bond in the substrate led to a high reactivity. It is postulated that catalytic oxidation on platinum catalysts proceeds

via initial rupture of the weakest C–H bond in the substrate followed by further reaction steps which involves free radical chemistry.

Chaiyasit (2000) investigated the selective oxidation reaction of 1-propanol and 2-propanol over Co-Mg-O/TiO_2 (8wt%Co, 1wt%Mg) catalyst. It was found that the oxidation property of Co-Mg-O/TiO_2 catalyst depended on type of the reactants. Propionaldehyde was the main product for selective oxidation of 1-propanol. In case of 2-propanol oxidation reaction, it was found that Co-Mg-O/TiO_2 catalyst was an active catalyst for the selective oxidation reaction. The main product at low reaction temperature was propylene while at high reaction temperature the main reaction products were propylene and propionaldehyde. From the result of propylene oxidation, it could be indicated that propionaldehyde was produced directly from propylene. In addition, the sequence of cobalt and magnesium loading had no effect on the structure and catalytic performance of this catalyst. While the type of support affected the selectivity of supported cobalt catalyst.

Brink *et al.* (2000) studied the catalytic combustion of chlorobenzene on a 2 wt.% Pt/γ-Al_2O_3 catalyst in binary mixtures with various hydrocarbons (toluene, benzene, cyclohexane, cyclohexene, 1,4-cyclohexadiene, 2-butene, and ethene) and with carbon monoxide. For all binary mixtures used they repoeted that the excess of added hydrocarbon increased the rate of conversion of chlorobenzene. With 2-butene, temperature at which 50% conversion and temperature at which 100% conversion for chlorobenzene were reduced by 100 and 200°C, respectively. Toluene and ethene were almost equally efficient as 2-butene. Co-feeding benzene or carbon monoxide resulted in a much smaller decrease of the *T*50%. The additional heat and water production in hydrocarbon combustion may contribute to some extent to the observed rate acceleration, but removal of Cl from the surface due to the hydrocarbon appears to be the major factor. The co-feeding of hydrocarbons invariably reduced the output of polychlorinated benzenes, which are formed as byproducts in the combustion of chlorobenzene on Pt/γ-Al_2O_3. Again, especially toluene, ethene, and 2-butene were very efficient. Benzene as well as cyclohexane, cyclohexene, and 1,4-cyclohexadiene, which were converted in situ into benzene was much less effective, due to chlorination of the aromatic nucleus. In chlorobenzene CO mixtures the levels of

polychlorinated benzenes were almost as high as with chlorobenzene per se. Removal of Cl from the surface (mainly in the form of HCl) by (non-aromatic) hydrocarbons is responsible for reducing the formation of byproducts.

Deutschmann *et al.* (2000) studied hydrogen assisted catalytic combustion of methane on platinum experimentally and numerically. In the experiment, they measured the exit temperatures of methane/hydrogen/air mixtures flowing at atmospheric pressure through platinum coated honeycomb channels. A single channel of this monolith was investigated numerically by a two-dimensional Navier–Stokes simulation including an elementary-step surface reaction mechanism. Furthermore, a one-dimensional time-dependent simulation of a stagnation flow configuration is performed to elucidate the elementary processes occurring during catalytic ignition in the mixtures studied. The dependence of the hydrogen assisted light-off of methane on hydrogen and on methane concentrations was discussed. The light-off was primarily determined by the catalyst temperature that was a result of the heat release due to catalytic hydrogen oxidation. Increasing hydrogen addition ensures light-off, decreasing hydrogen addition requires an increasing methane feed for light-off.

Minicò *et al.* (2000) investigated catalytic oxidation of 2-propanol, methanol, ethanol, acetone and toluene on coprecipitated Au/Fe_2O_3 catalysts in the presence of excess of oxygen. Gold catalysts have been found to be very active in the oxidation of tested volatile organic compounds (VOCs). The high activity of these systems has been related to the capacity of highly dispersed gold to weaken the Fe–O bond thus increasing the mobility of the lattice oxygen which is involved in the VOCs oxidation probably through a Mars–van Krevelen reaction mechanism.

Tongsang (2001) studied the oxidation property of the V-Mg-O/TiO_2 catalysts on the combustion of phthalic anhydride and maleic anhydride. From the results, the MgO modified V_2O_5/TiO_2 catalysts could better oxidize the anhydride ring than the unmodified one. Additionally, the appropriate ratio of vanadium per magnesium led to a balance between the adsorption of the anhydrides and the catalytic activity of vanadium and titania support.

Umpo (2001) investigated the oxidation property of the Co-Mg-O/Al_2O_3 catalyst on the combustion of phthalic anhydride and maleic anhydride. The results showed that magnesium promoted the adsorption of anhydride leading to better combustion of the anhydrides. The research also found that the ratio of cobalt per magnesium should be at an appropriate ratio to keep a balance between the adsorption of the anhydrides and the catalytic activity of cobalt and alumina support.

Centeno *et al*. (2002) investigated the catalytic oxidation of n-hexane, benzene and 2-propanol on Au/CeO_2/Al_2O_3 and Au/Al_2O_3 catalysts. It was showed that ceria enhanced the fixation and final dispersion of gold particles, leading to stabilize them in lower crystallite size. Catalytic results showed that ceria improved the activity of gold particles in the oxidation of the tested volatile organic compounds (VOCs) probably by increasing the mobility of the lattice oxygen and controlling and maintaining the adequate oxidation state of the active gold particles.

Gervasini *et al*. (2002) investigated the catalytic combustion with and without pre-catalytic actions (i.e., ionisation/ozonisation (I/O)) of tetracloromethane over alumina-supported copper-chromite and manganese dioxide catalysts with and without the presence of hydrogen-rich compounds, i.e. *n*-hexane and toluene,was evaluated. Experiments were performed at conditions of lean carbon tetrachloride concentration (from 500 to 3000 ppm v) in excess air, between 100 and 500 $^{\circ}$C in a continuous reaction line at laboratory scale. *n*-Hexane and toluene were added to the feedstream in variable concentration, between 100 and 500 ppmv. Ionisation/ozonisation of pure CCl_4 streams and of streams of hexane or toluene admixtures showed the efficiency of the hydrogen donor role of the hydrocarbons on CCl_4 conversion. The tests of ionisation/ozonisation were performed at different residence times in the ionisation reactor and a rate equation with second-order in CCl_4 concentration was found to represent the ionisation process. Over Cu-Cr and Mn catalysts, both *n*-hexane and toluene improved the CCl_4 combustion when added at low concentration (ca. 300 $^{\circ}$C) but inhibited it when they were present at high concentration (ca. 350 $^{\circ}$C). Catalytic combustion assisted with ionisation process enhanced CCl_4 conversion at low temperatures in comparison with conventional catalytic combustion (e.g. 90% of 1000 ppmV of CCl_4–hexane mixture was converted

on Cu-Cr at 250 °C and 5000 h^{-1} by the combined actions of catalytic and ionisation processes). Selectivity to CO_2 was controlled on the two catalysts. Mn was more active but less selective than Cu-Cr catalyst. Various oxygenated and chlorinated by-products, in particular $COCl_2$, were formed during ionisation of CCl_4 streams. By-products were greatly reduced and $COCl_2$ disappeared at 250 °C on catalysts.

Dias *et al.* (2002) investigated the selective oxidation of *o*-xylene to phthalic anhydride (PA) on a series of ternary V-Ti-Si oxides. Fresh and used catalysts, containing one monolayer of V_2O_5 on TiO_2-SiO_2 supports with 0.5, 1, 2 and 3 monolayers of TiO_2 on SiO_2, were characterised by Raman spectroscopy, X-ray diffraction (XRD) and temperature-programmed reduction (TPR). The characteristics and catalytic behaviour of these catalysts were compared with those of catalysts containing one monolayer of V_2O_5 supported on SiO_2 and on TiO_2. In the ternary V-Ti-Si catalysts, the presence of V_2O_5 and TiO_2 (anatase) was detected, TiO_2 (rutile) being also found in those with two and three monolayers of TiO_2. The formation of TiO_2 (rutile) due to exposure to reaction conditions was not observed. A moderate rearrangement of surface vanadium oxide species into crystalline V_2O_5 is observed. In addition, the formation of V_2O_4 was detected by XRD in the used catalyst containing one monolayer of V_2O_5 on the support with one monolayer of TiO_2 on silica. The TPR of used and fresh samples showed that the reduction of vanadium occurs during reaction, such reduction being partially reversible after reoxidation in air flow at high temperature. This partial reduction may favour the aggregation of dispersed vanadia species into crystalline V_2O_5. The catalytic behaviour of ternary systems in the selective oxidation of *o*-xylene depended strongly on the characteristics of the support. An increase in the content of TiO_2 led to a decrease in the temperature required to achieve total conversion. The use of SiO_2 as support caused formation of large amounts of undesirable C_8 products, whereas the presence of TiO_2 deposited on SiO_2 led generally to the formation of lower amounts of such products. The formation of both CO_2 and tar was strongly favoured on the support composed of two monolayers of TiO_2 on SiO_2.

Kim (2002) studied the catalytic oxidation of aromatic hydrocarbons over supported metal oxide. The catalytic activity of metal (Cu, Mn, Fe, V, Mo, Co, Ni,

Zn)/γ-Al_2O_3 was investigated to bring about the complete oxidation of benzene, toluene and xylene. Among them, Cu/γ-Al_2O_3 was found to be the most promising catalyst from the viewpoint of activity. Increasing the calcination temperature resulted in decreasing the specific surface areas of catalysts, subsequently the catalytic activity. The copper loadings on γ-Al_2O_3 had a great effect on catalytic activity, and 5 wt% Cu/γ-Al_2O_3 catalyst was observed to be the most active. The activity of 5 wt% Cu/γ-Al_2O_3 with respect to the VOC molecule was observed to follow the sequence: toluene > xylene > benzene, indicating that the combination of the catalyst property and the physicochemical property of the reactant plays an important role in activity.

Nuampituk (2002) investigated the oxidation property of the Cr, Mn, Mo, W, Fe and Zn promoted MgO on Al_2O_3 supported catalysts on the combustion of phthalic anhydride. It was found that the loading sequence of the metal affected the catalytic activity by changing the number of the surface basic sites. The effects would be positive or negative depended on the type of transition metal and the amount of the magnesium selected. If the amount of magnesium selected was lower than the optimum amount, the procedure that resulted in a larger number of the surface basic site would yield a catalyst with higher catalytic activity. On the other hand, if the amount of magnesium selected was higher than the optimum amount, the procedure that resulted in a larger number of the surface basicity would decrease the catalytic activity.

Nugoolchit (2002) investigated the effects of MgO on the oxidation property of the transition metal oxide catalysts on the combustion of phthalic anhydride. The results showed that magnesium oxide promoted the adsorption of phthalic anhydride leading to better combustion of the phthalic anhydride for the acidic and amphoteric metal oxides. For the basic metal oxides, the magnesium oxide addition would decrease the combustion of phthalic anhydride. The research also found that the ratio of transition metal oxide per magnesium oxide should be at an appropriate ratio to keep a balance between the adsorption of the phthalic anhydride and the catalytic activity of the transition metal oxides.

Ordóñez *et al* (2002) investigated the catalytic oxidation of benzene, toluene and *n*-hexane in air, both alone and in binary mixtures, over a commercial Pt on γ-alumina catalyst. Studies have been carried out at concentrations of up to 4200 ppmV, in a laboratory fixed-bed catalytic reactor. Results for single compounds show that temperature at which 50% conversion is attained increases as concentration increases for benzene and toluene, while the opposite behavior is observed for *n*-hexane. Results for mixtures show that, while the presence of *n*-hexane does not affect the conversion of benzene and toluene, the presence of benzene or tolueneinhibits the combustion of hexane, and the aromatic compounds inhibits each other when are reacted together.

Anastasov (2003) studied the deactivation of an industrial V_2O_5-TiO_2 catalyst for the oxidation of o-xylene into phthalic anhydride. The industrial reactor investigated contained 10550 tubes of 26 mm inner diameter and 3250 mm length. The catalyst was loaded in the tubes, while a molten salt $NaNO_2/KNO_3$ circulating in the shell-side removed the heat generated by the reactions. The catalyst was a V_2O_5-TiO_2 (anatase) supported catalyst. The weight ratio V_2O_5/TiO_2 was 0.06, the catalyst being promoted by rubidium and phosphorus. The active substance (0.1 mm thick) was laid over porcelain ring in order to increase the contact surface. The sizes of a ring were height 6 mm, outside and inside diameters 8.4 and 4.6 mm, respectively. There were three to four pellets on a tube diameter. The length of the bed was 280 cm, while its bulk density was about 1500 kg/m^3. From the results, the very low activity of a catalyst being 60.5 months old in the region after 100 cm. of the bed, was most probably due to a reversible deactivation caused by tar products blocking the active site. Therefore, the catalyst must be removed after 5 years use.

Cimino *et al.* (2003) studied effect of the addition of a second fuel such as CO, C_3H_8 or H_2 on the catalytic combustion of methane over ceramic monoliths coated with $LaMnO_3$/La-γAl_2O_3 catalyst. Results of autothermal ignition of different binary fuel mixtures characterised by the same overall heating value show that the presence of a more reactive compound reduces the minimum pre-heating temperature necessary to burn methane. The effect was more pronounced for the addition of CO and very similar for C_3H_8 and H_2. Order of reactivity of the different fuels established in isothermal activity measurements was: $CO > H_2 \geq C_3H_8 > CH_4$. Under autothermal

conditions, nearly complete methane conversion was obtained with catalyst temperatures around 800 °C mainly through heterogeneous reactions, with about 60–70 ppm of unburned CH_4 when pure methane or CO/CH_4 mixtures were used. For H_2/CH_4 and C_3H_8/CH_4 mixtures, emissions of unburned methane were lower, probably due to the proceeding of CH_4 homogeneous oxidation promoted by H and OH radicals generated by propane and hydrogen pyrolysis at such relatively high temperatures. Finally, a steady state multiplicity was found by decreasing the pre-heating temperature from the ignited state. This occurrence were successfully employed to pilot the catalytic ignition of methane at temperatures close to compressor discharge or easily achieved in regenerative burners.

Graham *et al.* (2003) studied the effects of V/Ti mass ratios in nanostructured V_2O_5/TiO_2 catalysts on catalyst characteristics and catalyst activities were investigated. The destruction of monochlorobenzene was used as a measure of catalyst activity. The V_2O_5/TiO_2 catalysts, which have been traditionally used as de-NO*x* catalysts and selective oxidation catalysts (e.g. in the production of phthalic anhydride), were made by the wet incipient method. This synthesis method provided nanostructured V_2O_5/TiO_2 catalysts with the vanadium species on the surface of the TiO_2. The catalysts were characterized using X-ray diffraction (XRD), BET surface area, and Raman spectroscopy. The performance of the catalysts for the destruction of organic pollutants was assessed in a differential tube flow reactor for gas-phase thermal oxidation reactions. It was found that the presence of crystalline V_2O_5 on the surface of TiO_2 (V/Ti mass ratio 0.05 and 0.1) is necessary for the oxidation of monochlorobenzene at temperatures <300 ◦C.

López-Fonseca *et al.* (2003) studied the complete oxidation of 1,2-dichloroethane dichloromethane and trichloroethylene as individual chlorohydrocarbons and of their binary mixtures over protonic zeolites (H-ZSM-5, H-MOR and chemically dealuminated H-Y zeolite) using a conventional fixed bed flow reactor. Its catalytic performance was associated with the presence of strong Brönsted acidity. Both H-MOR and chemically dealuminated H-Y zeolites exhibited the highest destruction activity for the abatement of single and binary mixtures. The destruction of chlorinated mixtures induced an inhibition of the reactivity of each

compound leading to a significant increase in the ignition temperature, which varied form one compound to other. On the other hand, a moderate decrease in chlorinated intermediates/by-products formation was noted. Likewise, the presence of hydrogen, either as a part of the additional chlorinated molecule or as a part of water generated as a reaction product, was determined to be important for efficient combustion of the chlororganics to HCl.

2.2 Comment on previous works

- V_2O_5-TiO_2 catalyst

The reviewed literatures show that vanadium oxide supported on titanium oxide is widely employed in selective oxidation reactions, such as partial oxidation of o-xylene to phthalic anhydride and selective catalytic reduction of nitric oxide. Several studies have aim to improve activity and selectivity of catalysts [Dias *et al.* 2001, Amiridis *et al.* 1999 and Lietti *et al.* 1999]. Several studies deactivation of an industrial V_2O_5-TiO_2 catalyst [Mongkhonsi and Kershenbaum 1998, Anastasov 2003]. Some work also found that the V_2O_5-TiO_2 catalyst can be used for the destruction of organic pollutants [Graham *et al*. 2003].

- Catalytic combustion of VOC and phthalic anhydride

From the above reviewed literature, it could be seen that the transition metal oxides showed the high activity of oxidation the organic compounds [Spivey 1987, Busca *et al.* 1997, Larsson *et al.* 1997 and Kim 2002]. Furthermore, the result of the combustion of phthalic anhydride on Cr, Mn, Fe, Co, Ni, Cu, Zn, Mo and W promoted MgO on Al_2O_3 supported catalysts [Nugoolchit 2002] and V-Mg-O/TiO_2 [Tongsang 2001] showed that MgO could promote the adsorption of phthalic anhydride leading to better phthalic anhydride combustion for the acidic and amphoteric metal oxides. For the basic metal oxides, the magnesium oxide addition would decrease the combustion of phthalic anhydride. The research also found that the ratio of transition metal oxide per magnesium oxide should be at an appropriate ratio to keep a balance between the adsorption of the phthalic anhydride and the catalytic activity of the transition metal oxides.

- Mixture effect

Very little has been reported in the literature on research into the catalytic oxidation of mixtures as compared to the catalytic oxidation of individual component. Often, but not always, the catalytic reaction cannot be predicted solely from the behavior of the individual component [Brink *et al.* 1999, Brink *et al.* 2000,

Deutschmann *et al.* 2000, Gervasini *et al*. 2002, Ordóñez *et al.* 2002, Cimino *et al*. 2003, and López-Fonseca *et al*. 2003].

Accordingly, this thesis is interested in the effects of hexane addition on phthalic anhydride combustion over V_2O_5/TiO_2 catalyst impregnated with transition metal oxide and magnesium oxide.

CHAPTER III

THEORY

Catalytic oxidation can be categorized as complete oxidation and selective oxidation. Complete oxidation is the combustion of organic compounds to the combustion products; CO_2 and H_2O [Thammanonkul (1996)]. It is a practicable method for the elimination of organic pollutants in gaseous streams. The selective oxidation is the reaction between hydrocarbon and oxygen to produce oxygenates (such as alcohols, aldehydes, carboxylic acids which are produced from partial oxidation processes) or unsaturated hydrocarbons (such as ethane and propene which can be produced from oxidative dehydrogenation process) [Thammanonkul (1996)].

In studies on oxidative catalysis, commonly great attention is attached to the state of oxygen on the catalyst surface. A relative inert oxygen molecule is activated by interacting with the surface of an oxide catalyst. The main parameter determining oxygen reactivity on the catalyst is the energy of oxygen binding with the catalyst as a thermochemical characteristic. Correlation between rates of catalytic oxidation and oxygen binding energy on oxide catalysts have been established. The weaker the oxygen binding with the catalyst surface, the more efficient is complete oxidation with this catalyst [Satterfield (1980)].

With oxide catalysts, chemisorbed surface oxygen as well as lattice oxygen may play a role. The oxidation of propylene to acrolein on a $BiMo/SiO_2$ catalyst in a pulsed reactor showed that surface chemisorbed oxygen as well as lattice oxygen could contribute to the overall reaction. It seemed plausible that in many other cases chemisorbed oxygen would lead to a different set of products than lattice oxygen and both mechanisms could be significant. On the basis of other studies advanced the hypothesis that surface-adsorbed oxygen may in general lead to products of complete oxidation and the lattice oxygen is needed for partially oxidized products [Satterfield (1991)].

3.1 Mechanism of oxidation reaction

The mechanism of oxidation reaction between a reactant and an adsorbed surface oxygen species on a catalyst surface can be shown as follows:

Reactant (fluid phase) → Reactant (surface species)

Oxygen (fluid phase) → Oxygen (surface species)

Reactant (surface species) + Oxygen (surface species) → Product (surface species)

Product (surface species) → Product (fluid phase)

3.2 Magnesium promoted transition metal oxide catalysts

Transition metal oxides were interesting materials in the field of heterogeneous catalysis. The most active single metal oxide catalysts for complete oxidation for a variety of oxidation reactions were usually found to be oxides of V, Cr, Mn, Fe, Co, Ni, and Cu. For the complete oxidation of methane, methanol, ethanol, acetaldehyde, and ethanol/methanol mixture, the transition metal oxide catalysts exhibited high activity. The $CuMn_2O_4/Al_2O_3$ catalyst was more active than the CuO_x/Al_2O_3 and Mn_2O_3/Al_2O_3 catalyst for the complete oxidation of CO, ethyl acetate, and ethanol. The MoO_3/SiO_2 was the most active catalysts among the MoO_3/support catalysts for the diesel soot oxidation. For the photo-oxidation of benzoic acid, TiO_2/W was the most efficient catalyst.

MgO was white powder that usually obtained by dehydration of magnesium dihydroxide. Its catalytic interest lied in its essentially basic surface character, which made it an effective catalyst support. Magnesium oxide was interesting because it had the ability to stabilize metals in unusual oxidation states and to avoid sintering and evaporation of the metal atoms [Aramendia *et al*. (1999)].

3.3 Acidic and Basic Catalyst [Kirk-Othmer (1979)]

The correlation of catalytic efficiency with the strength of the acid or base was of considerable importance. The general theory of acid-base catalysis in which a proton is transferred from the catalyst to the reactant (acid catalysis) or from the reactant to the catalyst (base catalysis). The velocity of the catalyzed change is thought to be determined by a protolytic reaction between the reactant and the catalyst. The molecule, on receiving or giving a proton, is converted into an unstable state which immediately (or very rapidly, compared with the velocity of the protolytic reaction) leads to the reaction under consideration. Thus, acid catalysis of a basic reactant is represented by the general scheme $R+AH^+ \rightarrow RH^+ + A$, whereas $RH^+ + B \rightarrow R+BH^+$ represents basic catalysis of an acidic reactant.

3.4 Chemisorption at oxide surface [Bond (1987)]

On the basis of their electrical conductivities, solids are traditionally divided into four classes as shown in Table 3.1.

Table 3.1 Classification of solids by electrical conductivity

Class	Conductivity range (Ω cm^{-1})	Chemical class	Examples
Superconductors	up to 10^{35}	metals at low temperatures	-
Conductors	10^4-10^6	metals and alloy	Na, Ni, Cu, Pt etc.
Semiconductors	10^3-10^8	(a) intrinsic: semi-metals	Ge, Si, Ga, As etc.
		(b) extrinsic: oxides and sulphides of transition and post-transition elements	ZnO,Cu_2O, NiO, ZnS,MoS_2, NiS etc.
Insulators	10^{-9}-10^{-20}	Stoichiometric oxides	MgO, SiO_2, Al_2O_3 etc.

Of greater interest are the oxides and sulphides whose conduction is due to their departure from precise stoichiometry: these substances are termed *extrinsic* or defect semiconductors. The more non-stoichiometric they are, the greater their conductivity. Another important general feature of semiconductors is that their conductivity increases with temperature according to a relation similar to the Arrhenius equation.

A useful generalization concerning the requirement for p-type semi-conductivity is that the cation shall have an accessible higher oxidation state: thus cobalt(II)oxide and copper(I)oxide are also in this group. For n-type semiconductivity an accessible lower oxidation state (which may include the zero-valent state) is needed: thus cadmium oxide and iron(III)oxide fall in this group (see Table 3.2).

Table 3.2 Classification of semiconducting metal oxides

Effect of heating in air	Classification	Examples
Oxygen lost	Negative (n-type)	ZnO, Fe_2O_3, TiO_2, CdO, V_2O_5, CrO_3, CuO
Oxygen gained	Positive (p-type)	NiO, CoO, Cu_2O, SnO, PbO, Cr_2O_3

3.4.1 Chemisorption on semiconducting oxides

A qualitative understanding of the chemisorption of simple gases on semiconducting oxides follows simply from their chemistry. Reducing gases such as hydrogen and carbon monoxide are adsorbed strongly, but irreversibly: on heating, only water and carbondioxide respectively can be recovered. Hydrogen probably dissociates heterolytically on adsorption, viz.

$$H_2 + M^{2+} + O^{2-} \rightarrow HM^{+} + OH^{-}$$

The hydroxyl ion will decompose on heating to form water and anion vacancies, and an equal number of cations will be reduced to atoms.

Carbon monoxide usually chemisorbed first on the cation, whence it reacts with an oxide ion:

$$(CO) \bullet\bullet\bullet M^{+} + O^{2-} \rightarrow M + CO_2.$$

Here is the first stage of a process that can lead ultimately to the complete reduction of the oxide to metal. These steps are also similar to those involved in the catalyzed oxidation of these molecules.

The chemisorption of oxygen on p-type oxides occurs by a mechanism involving the oxidation of Ni^{2+} ions at the surface to Ni^{3+}:

$$2Ni^{2+} + O_2 \rightarrow 2(O^{-} \bullet\bullet\bullet Ni^{3+}).$$

High coverages by the O^{-} ion can result, and it is easy to see that this is the first step in the incorporation of excess oxygen, referred to above. When the n-type oxides (exemplified by zinc oxide) are exactly stoichiometric, they cannot chemisorb oxygen: when however they are oxygen-deficient, they can chemisorb just as much as is needed to restore their stoichiometry by refilling the anion vacancies and reoxidizing the zinc atoms.

3.4.2 Adsorption on insulator oxides

Since the cations of insulator oxides can be neither oxidized nor reduced, they cannot chemisorb oxygen to any significant extent; they cannot chemisorb hydrogen or carbon monoxide for the same reason. They can, and do, react with water and other polar molecules as:

$$M^{x+} + O^{2-} \xrightarrow{H2O} (HO^{-} \bullet\bullet\bullet M^{x+}) + OH^{-}$$

$$M^{x+} + O^{2-} \xrightarrow{CH3OH} (CH_3O^{-} \bullet\bullet\bullet M^{x+}) + OH^{-}$$

Indeed under normal circumstances the surface of oxides such as alumina and silica are covered by a layer of chemisorbed water: the surface is then said to be fully

hydroxylated, and indeed these hydroxyl groups are very firmly bound. Their complete removal by heating is almost impossible. When the oxides are suspended in water the M-OH groups can dissociate either as acids or as bases, depending on the electronegativity of the cation, e.g.

$$Mg - OH \rightarrow Mg^{2+} + OH^{-}$$

$$Si - OH \rightarrow SiO^{-} + H^{+}$$

The variation of valence electron quantity causes the oxidation number change. These phenomenon leads to the electrical conductivity and acidity change (consider in case of Lewis acid).

CHAPTER IV

EXPERIMENTAL

The experimental systems and procedures used in this work are divided into three parts:

1. The preparation of catalysts.
2. The characterization of catalysts.
3. The catalytic activity measurements.

The details of the experiments are described as the following.

The scope of this study

The reaction conditions are chosen as follows:

Catalysts	:	Cu- V-Mg-O/ TiO_2, Fe- V-Mg-O/TiO_2, Mo- V-Mg-O/ TiO_2, Zn-V-Mg-O/ TiO_2
Reactant	:	0.01% mol $C_8H_4O_3$ and 0.24% mol C_6H_{14}
Flow rate of reactant	:	100 ml/min
Reaction temperature	:	200-500°C
Space velocity	:	60000 ml $g^{-1}h^{-1}$

4.1 Preparation of catalysts

4.1.1 Chemicals

The details of chemicals used in this experiment are shown in Table 4.1.

Table 4.1 The chemicals used in this experiment.

Chemical	Grade	Supplier
Ammonium molybdate ($(NH_4)6Mo_7O_{24}\cdot 4H_2O$)	Analytical	Univar, Australia
Cupric nitrate trihydrate ($CuN_2O_6\cdot 3H_2O$)	Analytical	Fluka, Switzerland
Ferric nitrate nonahydrate ($FeN_3O_9\cdot 9H_2O$)	Analytical	Fluka, Switzerland
Magnesium nitrate ($Mg(NO_3)_2$)	Analytical	Fluka, Switzerland
Zinc nitrate hexahydrate ($ZnN_2O_6\cdot 6H_2O$)	Analytical	Fluka, Switzerland
Titanium oxide (TiO_2)	JRC-TIO1	Department of Material Science, Shimane University
Ammonium metavanadate ($NH_4(VO_3)$)	Analytical	Carlo Erba, Italy
Phthalic Anhydride ($C_8H_4O_3$)	Analytical	Fluka, Switzerland
Hexane (C_6H_{14})	Analytical	Univar, Australia

4.1.2 Preparation of catalyst

Each catalyst was prepared by 2 steps. In the first step V_2O_5/TiO_2 was prepared by wet impregnation. TiO_2 powder was added to an aqueous solution of ammonium metavanadate ($NH_4(VO_3)$) at 70°C. The suspension was evaporated at 80°C, then dried in the oven at 110°C in air over night. The resulting solid was calcined in air at 550°C for 6 hours. Then the desired metal (Fe, Cu, Zn or Mo) and magnesium was introduced into the calcined solid by co-impregnation from an aqueous solution containing both salt of a desired metal and magnesium nitrate $Mg(NO_3)_2$, evaporated at 80°C and dried at 110°C in air overnight. After drying the catalyst was calcined in air at 550°C for 6 hours.

4.2 The characterization of catalysts

4.2.1 Determination of composition content of catalysts

The actual composition contents of all the catalysts were determined by atomic absorption spectroscopy (AAS) at the Department of Science Service Ministry of Science Technology and Environment. The calculation of the sample preparation is shown in Appendix A.

4.2.2 BET Surface area measurement

- Apparatus

The apparatus consisted of two gas feed lines for helium and nitrogen. The flow rate of gas was adjusted by means of a fine-metering valve. The sample cell was made from pyrex glass. The BET surface areas were calculated from the amount of the adsorbed N_2. The amount of the adsorbed N_2 was measured using a gas chromatograph (GC GOW-MAC). The operation conditions of the gas chromatograph (GOW-MAC) is shown in Table 4.2.

Table 4.2 Operation conditions of gas chromatograph (GOW-MAC)

Model	**GOW-MAC**
Detector	TCD
Helium flow rate	30 ml/min
Detector temperature	80°C
Detector current	80 mA

- Procedure

The mixture of helium and nitrogen gas was flowed through the system at the nitrogen relative gauge pressure of 0.3. The sample was placed in the sample cell, which was then heated up to 150°C and held at this temperature for 2 h. The sample was cooled down to room temperature and ready to measure the surface area. There were three steps to measure the surface area.

(1) Adsorption step

The sample cell was dipped into the liquid nitrogen. Nitrogen was adsorbed on the surface of the sample until equilibrium was reached.

(2) Desorption step

The nitrogen-adsorbed sample was dipped into a water bath at room temperature. The adsorbed nitrogen was desorbed from the surface of the sample. This step was completed when the recorder line return back to the base line.

(3) Calibration step

1 ml of nitrogen gas at atmospheric pressure was injected at the calibration port and the area was measure. The area was the calibration peak. The BET surface area was calculated using procedures described in Appendix C.

4.2.3 X-ray diffraction (XRD)

The phase structures of the samples were determined by X-ray diffraction, Siemens D 5000 X-ray diffractometer using CuKα radiation with Ni filter in the 2θ range of 10-80^{o}. The sample was placed into XRD plate before placing on the measured position of XRD diffractometer.

4.2.4 Pyridine Adsorption

The acid site of the samples were determined by the pyridine adsorption. The apparatus consisted of the tube connected to the gas chromatograph (GC9A). The condition of the gas chromatograph is shown in Table 4.3.

Table 4.3 Operation conditions of gas chromatograph (GC9A) for pyridine adsorption

Model	GC9A
Detector	FID
Nitrogen flow rate	30 ml/min
Column temperature	150°C
Detector temperature	180°C
Injector temperature	180°C

0.02 g of sample was placed in the tube. 0.01 μl of pyridine was injected to the gas chromatograph and the peak area was measured. The pyridine was injected until the sample was saturated. The acid site of the sample was calculated from the total peak area of the pyridine adsorbed. The pyridine adsorption was calculated using the procedures described in Appendix G.

4.2.5 Maleic anhydride Adsorption

The basic site of the samples were determined by the maleic anhydride adsorption. The apparatus consisted of a tube connected to the gas chromatograph (GC9A). The condition of the gas chromatograph is shown in Table 4.4.

Table 4.4 Operation conditions of gas chromatograph (GC9A) for maleic anhydride adsorption

Model	GC9A
Detector	FID
Nitrogen flow rate	30 ml/min
Column temperature	280°C
Detector temperature	300°C
Injector temperature	300°C

0.03 g of sample was placed in the tube. 0.03 μl of maleic anhydride aqueous solution of known concentration (0.104 g/ml) was injected to the gas chromatograph and the peak area was measured. The maleic anhydride was injected until the sample was saturated. The basic site of the sample was calculated from the total peak area of the maleic anhydride adsorbed. The maleic anhydride adsorption was calculated using the procedures described in Appendix G.

4.2.6 FT-IR pyridine adsorption

4.2.6.1 Chemicals and reagents

Ultra high purity (99.99%) nitrogen suppies by TIG Ltd. and pyridine, analytical grade supplied by Univax or Ajax chemical were used in these experiment.

4.2.6.2 Instruments and apparatus

Flow diagram

The schematic diagram of the *in situ* FT-IR apparatus is depicted in Figure 4.1 All gas lines, valves and fittings in this apparatus were made of pyrex glass except the IR gas cell and the sample disk holder, which were made of quartz glass in order to avoid the adsorption of any glass species which may remain on the inner surface of glass tube while the system was evacuated. Nitrogen was used for purging before starting the experiment. Pyridine was added to a glass tube connected which a value which can open to the glass line system. A home made electro-magnetic pump, fixed in the gas line, was used for circulating the gas (including the pyridine vapour) through the sample in order to accomplish the adsorption of gas or pyridine species on the sample surface. A Labconco 195-500 HP vacuum pump, which theoretically had capacity at 10^{-4} Torr, was used for system evacuation. Furthermore, a digital pressure indicator, attached to the gas line, measured the pressure of the system and checked leaking of the apparatus as well.

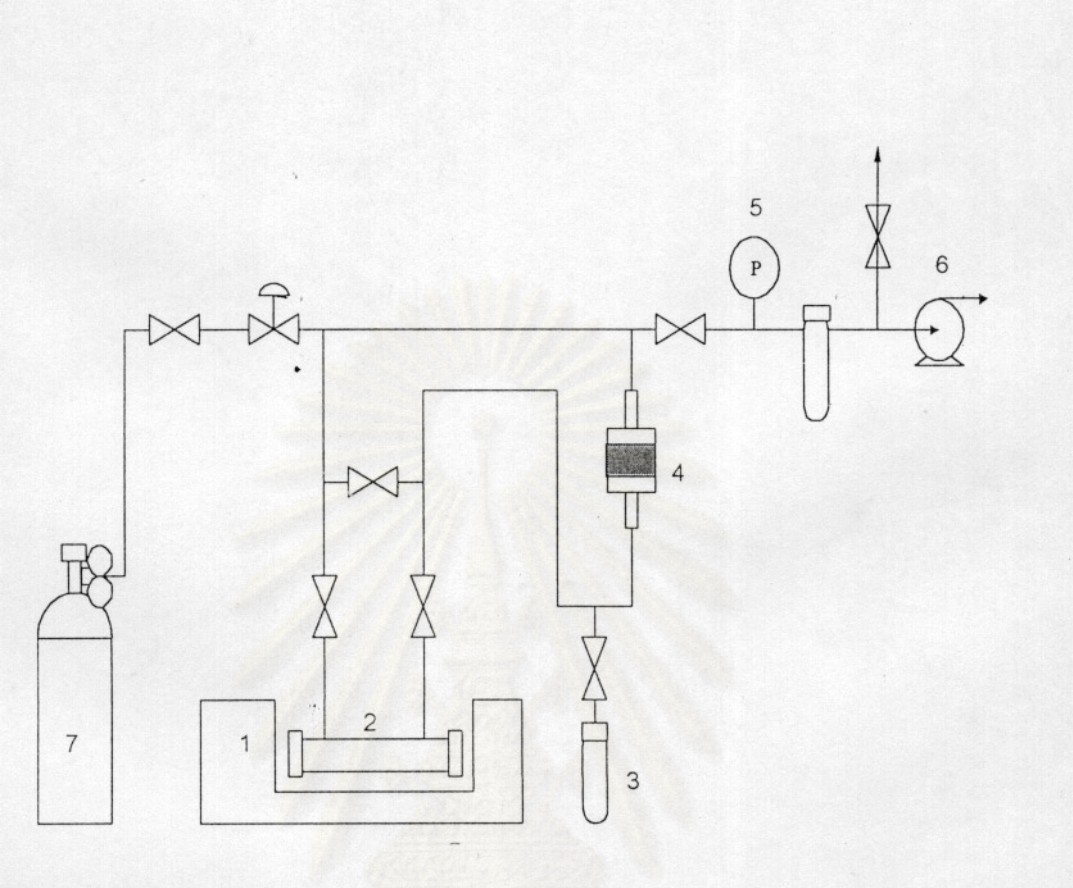

1. FT-IR Analyzer
2. IR quartz gas cell
3. Pyridine tube
4. Electro magnetic circulating pump
5. Digital pressure indicator
6. Vacuum pump
7. Nitrogen gas cylinder

Figure 4.1 Flow diagram of instrument used for pyridine adsorption experiment

FT-IR

The FTIR spectrometer was used as a detector in the experiments. A Nicolet model Impact 400 FT-IR equipped with a deuterated triglycine sulfate (DTGS) detector and connected to a personal computer with Omnic version 1.2a on Windows software (to fully control the functions of the IR analyser) were applied to this study. The analyzer was place on a moveable table for conveniently adjustment.

IR gas cell

The IR gas cell used in this experiment, shown in Figure 4.2, was made of quartz and covered with 32×3 mm NaCl windows at each end of the cell. Each window was sealed with two O-rings and a stainless flange fastened by a set of screws.

The cell is roughly divided into two zones; heating and cooling respect to their temperature. The function of the heating zone at the middle of the IR cell is the increase the temperature for the sample disk. The quartz sample holds for the sample disk to keep it perpendicular to the IR beam, is arranged inside the IR cell in the heating zone. A thermocouple is used to measure the sample disk temperature. The temperature is controlled by a variable voltage transformer and a temperature controller. At both end of the IR cell were cooled water. They were applied to reduce the excessive heating, which may damage O-ring seals and the windows.

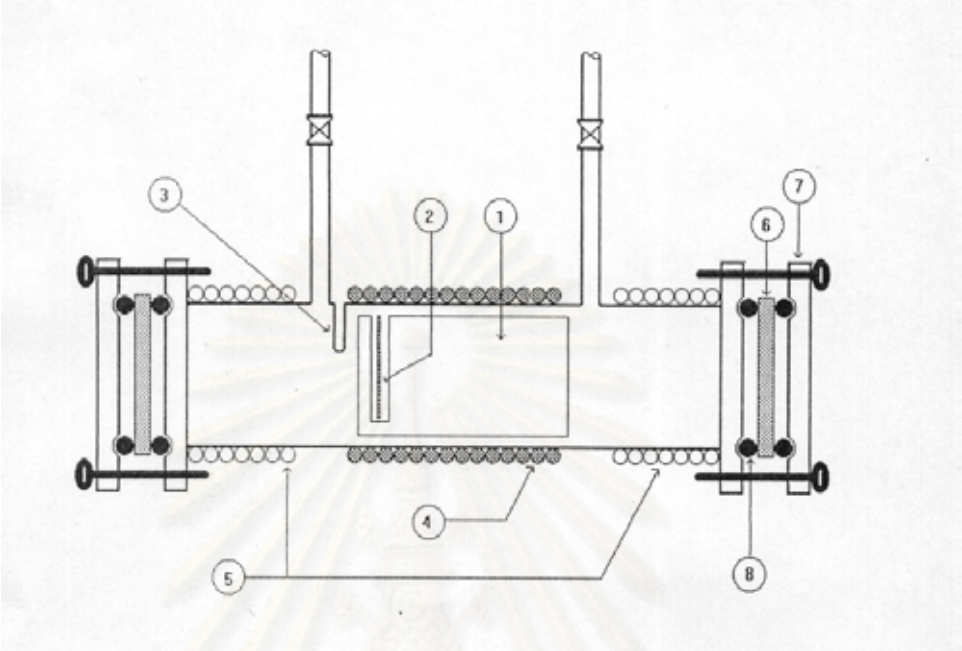

1. Sample Holder
2. Sample Disk
3. Thermocouple Position
4. heating rod
5. Water Cooling line
6. KBr Window
7. Flange
8. O-ring

Figure 4.2 IR gas cell used for pyridine adsorption experiment

4.2.6.3 Sample disk preparation

To produce a self-supporting catalyst sample disk for an IR experiment the catalyst was milled thoroughly in a small quartz mortar to obtain a very fine powder. This minimized the scattering of infrared radiation and provided a high quality of spectrum.

The die used was made of stainless steel and is shown in figure 4.3. The most important part of this die, which is directly in contact with the sample is the so-called the support disks. The support disks are composed of upper and lower disks, each 20 mm. in diameter. The support disks are highly polished to a mirror like finish in order to overcome the sticking of sample to the surface of the die, the main problem in pressing disks. The powder sample, about 0.055-0.065g, was spread to totally cover the surface of the lower support disk placed in the die to make the sample disk. If a thick sample disk was used, a poor IR would scan result and if too thin sample dick was employed, it would be easily cracked by thermal treating as well as broken itself. All part of die were put together and were pressed by a manual hydraulic press at pressure of 150-170 Kg/cm^2 for 5 minutes. The pressure should not be low so that a self-supporting disk cannot form. After pressing, the well-formed disk was carefully removed from the die and mounted in the IR cell.

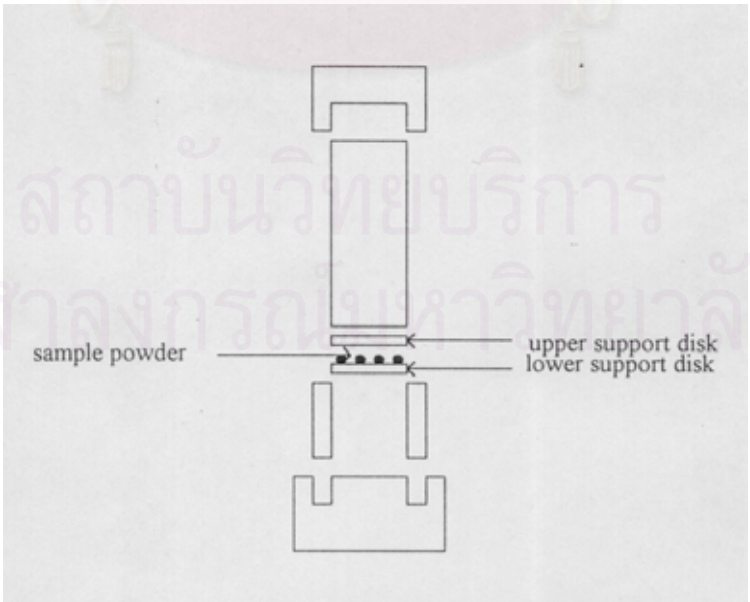

Figure 4.3 Body f the die for preparation of a self-supporting catalyst disk

4.2.6.4 Experimental procedure

After a well-formed sample disk is obtained, the sample disk was placed in the sample holder and then the sample holder, including the sample disk, was placed into the middle of IR gas cell. The sample disk is located as close to the thermocouple probe hole as possible. Once the KBr windows were sealed of the both end of the IR gas cell and the leaks were not observed, the IR gas cell was evacuated by a vacuum pump through the gas line for at least 30 minutes to place the system under vacuum. The sample disk was evacuated in vacuum for 1 hour at room temperature. However, since no change of the IR spectrum of the sample was found during the pre-treatment, this step something ignored. Pyridine vapour was brought into contact with the disk at room temperature. Under vacuum, liquid pyridine evaporates from the pyridine tube in to the gas line leading to the IR gas cell. To achieve the maximum adsorption of pyridine, pyridine vapour was circulated though the system by the electro-magnetic pump for 1 hour or until the IR spectrum of pyridine peak did not change. After that, the IR cell and gas line were evacuated to remove not only pyridine vapour remaining in the cell and gas line but also the physisorbed pyridine from the catalyst surface too. The vacuum pump was operated until the IR spectra peaks of pyridine vapour and physisorbed pyridine totally vanished and there was no change in any other peaks of the spectra. This normally took around 1.5 hours then, FT-IR measurement of the spectra of the pyridine-adsorded sample started at room temperature and was repeated at elevated temperature in 50 C steps.

The vacuum pump was kept running while the sample disk and the IR gas cell were heating to remove all species desorbed from the sample surface out of the system in order to avoid disturbing the result spectra by such species. On the other hand, since the vibration would occur and bring about bad scans, the vacuum was switched off while the temperature was held constant for IR detection. The measurement was completed when all peaks of adsorbed pyridine disappeared so that the IR spectra of the sample was identical to the one before pyridine dosing

4.3 The catalytic activity measurements

4.3.1 Equipment

The combustion system, as shown in Figure 4.4., consists of a reactor, two saturators, an automatic temperature controller, an electrical furnace and a gas controlling system.

The reactor is made from a stainless steel tube (O.D. 3/8"). Sampling points are provided above and below the catalyst bed. Catalyst is placed between two quartz wool layers.

An automatic temperature controller consists of a magnetic contractor model Telex 87114. Reactor temperature was measured at the bottom of the catalyst bed in the reactor. The temperature control set point is adjustable within the range of 0-800°C at the maximum voltage output of 220 volt.

The electrical furnace supplies heat to the reactor for phthalic anhydride combustion. The reactor can be operated from room temperature up to 800°C at the maximum voltage of 220 volt.

The gas supplying system consists of cylinders of air zero, each equipped with pressure regulators (0-120 psig), on-off valves and fine-meter valves used for adjusting the flow rate.

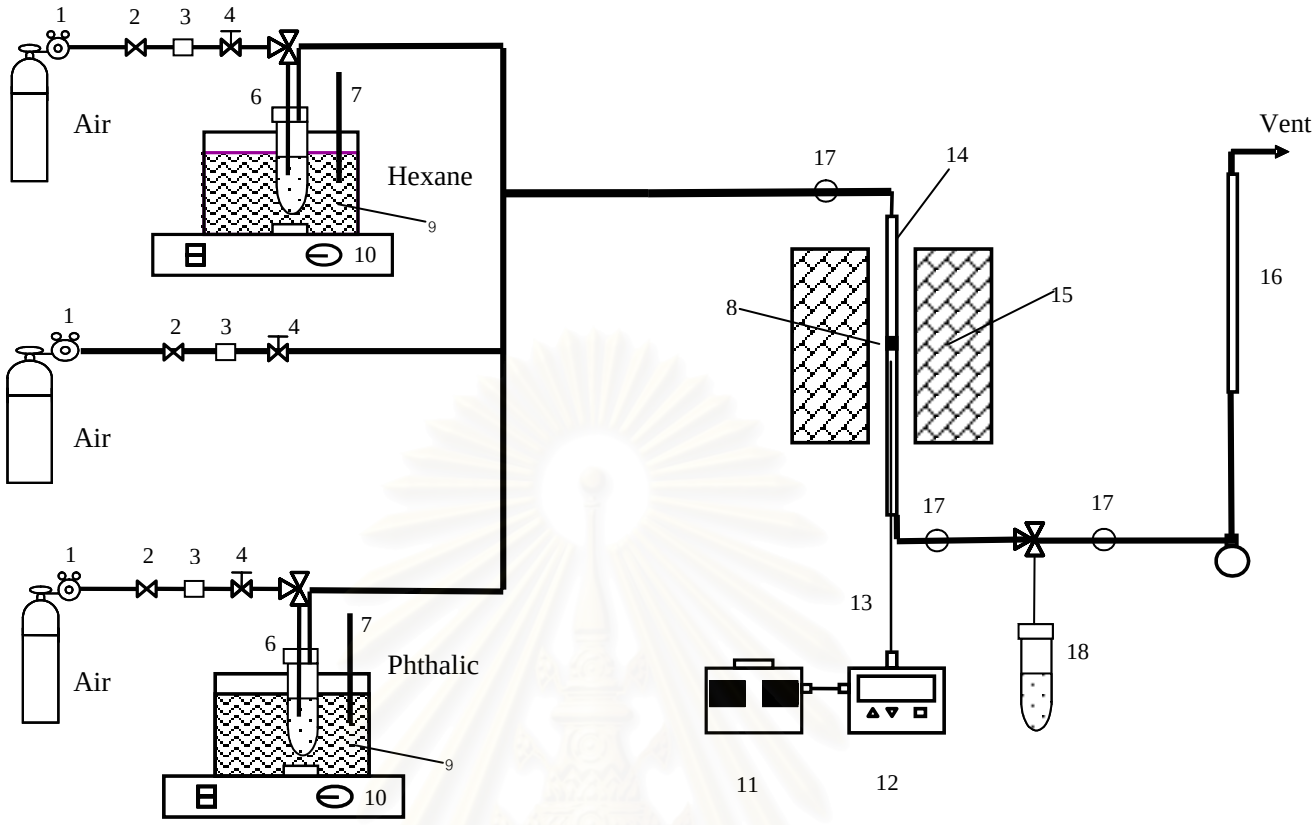

1. Pressure Regulator	2. On-Off Valve	3. Gas Filter
4. Metering Valve	5. Heating Line	6. Saturator
7. Thermometer	8. Catalyst Bed	9. Sand
10. Stirring Controller	11. Variable Voltage Transformer	12. Temperature Controller
13. Thermocouple	14. Reactor	15. Furnace
16. Flow Meter	17. Sampling Point	18. Tap

Figure 4.4 Flow diagram of phthalic anhydride combustion system

The composition in the feed and product stream was analyzed by flame ionization detector gas Chromatograph Shimadzu GC9A.

A Shimadzu GC8A gas chromatograph equipped with a thermal conductivity detector was used to analyze permanent gases and water. Two columns, a 5A molecular sieve to separate oxygen and CO and a Porapak-Q column to separate CO_2 and water were operated in parallel. The operating conditions of the GC are listed in the Table 4.5.

Table 4.5 Operating conditions for gas chromatographs

Gas chromatograph	**GC8A**	**GC9A**
Detector	TCD	FID
Column	MS-5A, Porapak-Q	Chromosorb WAW
Carrier gas	He (99.999%)	N_2 (99.999%)
Carrier gas flow	25 ml/min	30 ml/min
Column temperature	100°C	210°C
Detector temperature	130°C	250°C
Injector temperature	130°C	250°C
Analyzed gas	CO, CO_2, H_2O	$C_8H_4O_3$ and C_6H_{14}

4.3.2 Oxidation procedure

The oxidation procedures are described in the detail below.

1. 0.1 gram of catalyst was packed in the middle of the stainless steel microreactor located in an electrical furnace.
2. The total flow rate was 100 ml/min. The concentration of phthalic anhydride and hexane in air was adjusted to the required values.
3. The reaction temperature was between 200-500^{o}C. The effluent gas was analyzed by using the FID and TCD gas chromatograph. The chromatograph data were changed into mole of phthalic anhydride, haxane and CO_2 by calibration curves in Appendix D.

The operating conditions selected have been checked to confirm that there was no external and internal mass transfer resistance. The calculation was shown in Appendix B.

CHAPTER V

RESULTS AND DISCUSSION

The results and discussion in this chapter are divided into two major parts including the catalyst characterization and the catalytic combustion reaction of phthalic anhydride, and surface acidity and basicity, respectively.

5.1 Catalyst characterization

5.1.1 Determination of composition content and BET surface area of catalyst

The results of metal composition and BET surface area of all catalysts, which were analyzed by atomic absorption spectroscopy (AAS) and BET surface area are summarized in Tables 5.1.

Table 5.1 The composition of different magnesium loading catalysts and BET surface area

Catalyst	wt% metal	wt% Mg	BET surface area (m^2/g)
TiO_2	-	-	50.64
8Cu- 7V-1Mg-O/TiO_2	7.9	1.00	7.88
8Fe- 7V-1Mg-O/TiO_2	7.7	1.10	12.22
8Mo- 7V-1Mg-O/TiO_2	6.3	0.94	8.99
8Zn- 7V-1Mg-O/TiO_2	6.8	1.00	7.12

It must be noted here that the amounts of the transition metals and magnesium used in this work have not been proved to be the amounts that yielded the best performance catalyst for each transition metal. The previous works [Nuampituk (2002), Nugoolchit (2002)] have showed that adding about 1wt% Mg could

signiticantly increase the combustion activity of the catalysts. Mg loading higher than 1wt% may increase or decrease the combustion activity. In case of activity gain, the increase of Mg loading from 1wt% to 4wt% did not strongly increase of the combustion activity as the increase from 0wt% to 1wt%. Therefore, 1wt% Mg was choosen in this work. The amount of the transition metals was fixed at 8 wt% to make the obtained results comparable to the previous works [[Nuampituk (2002), Nugoolchit (2002)].

5.1.2 X-ray Diffraction (XRD)

The first three strongest XRD peaks of transition metal oxides from the reference [The JCPDS (1980)] using CuKα radiation are listed in Table 5.2.

Table 5.2 The reference XRD patterns for transition metal oxides

Oxides	Position (2θ)	Oxides	Position (2θ)
CuO	35.4°, 35.6°, 38.8°	MoO_3	9.6°, 25.8°, 29.4°
Cu_2O	37°, 40.4°, 42.4°	MoO_2	26°, 36.8°, 53.4°
Fe_2O_3	29.8°, 32.8°, 67.5°	ZnO	33.6°, 58.4°, 62.6°
FeO	61°, 61.4°, 73°	ZnO_2	31.8°, 37°, 63°
MgO	37°, 43°, 62.8°		

XRD was used to determine the bulk crystalline phases in the catalysts. The diffraction patterns of all catalysts are shown in Fig 5.1. The XRD pattern of TiO_2 showed strong diffraction peaks at 25.3°, 37.8°, 48.0°, 53.9° and 55.1° indicating the TiO_2 is in the anatase form.

From the XRD result of V_2O_5/TiO_2, it was observed that only peaks of TiO_2 were present in the XRD pattern. The peak of vanadium oxide was not detected possibly because the XRD pattern of vanadium oxide was hidden by the XRD pattern of TiO_2 support, or vanadium oxide did not form a crystal with significant size or did not form a crystal. It was also found that the TiO_2 (anatase) support did not undergo

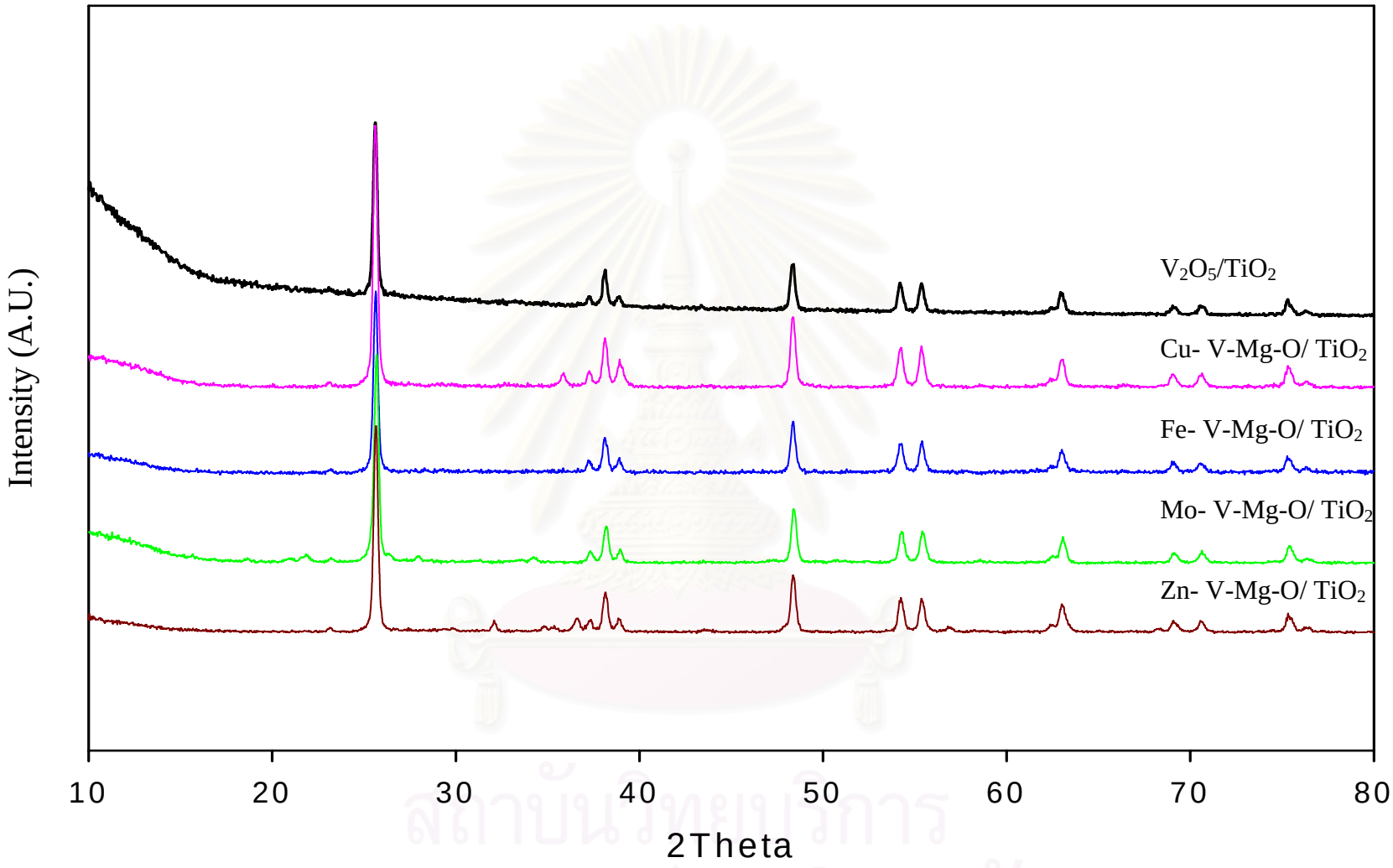

Figure 5.1 The XRD pattern of all catalysts

structural changes during the vanadia impregnation and calcinations (550°C-6 hr) in the first step because the XRD analysis only exhibited the anatase phase (rutile was not present in the XRD pattern).

After addition of Fe, Cu, Zn and Mo in the second step, different results were observed. The XRD result of Cu-V-MgO/TiO_2 showed two small diffraction peaks at 35.8° and 38.6° which are belong to CuO.

For Zn-V-MgO/TiO_2, the introduction of zinc oxide induced the appearance of small peaks of ZnO. These peaks were very weak at 31.9° and 36.4°. The relative intensity of those peaks was much lower compared to the TiO_2 peaks. This observation suggested that CuO and ZnO could form crystal with significant size on the catalyst surface.

Similar diffraction patterns were obtained for Fe-V-MgO/TiO_2 and Mo-V-MgO/TiO_2. The XRD results of Fe and Mo showed only the TiO_2 peaks and did not show any peak of these transition metal oxides. The peaks of Fe and Mo oxides were not detected possibly because the XRD patterns of these transition metal oxides were hidden by the XRD pattern of TiO_2 support, the oxides did not form a crystal with significant size or it did not form a crystal.

5.2 Activity and surface acidity/basicity

The surface acidity and basicity of the catalysts can be quantitatively measured by the amount of pyridine and maleic anhydride adsorption, respectively. The large amount of pyridine adsorption implies the large numbers of acid sites. The large amount of maleic anhydride adsorption implies the large numbers of basic sites. The maleic anhydride also indicated the ability of adsorption of the acidic reactant, phthalic anhydride. Thus, the large amount of maleic anhydride adsorption would have the large numbers of adsorption sites.

From the hypothesis in the previous works [Tongsang(2001), Umpo(2001), Nugoolchit (2002)], the acid site was the active site. The basic site (MgO) would help the adsorption of the acidic reactant, but in the same time, these basic sites would neutralize the acid site (active site). Thus, the maximum activity of the phthalic anhydride combustion needed the optimum between the adsorption of the phthalic anhydride and the catalytic activity of the transition metal oxides.

5.2.1 Pyridine and maleic anhydride adsorption

The amount of pyridine and maleic anhydride adsorption related to the TiO_2 and the amounts of absorbed pyridine and maleic anhydride of acidic metal oxides are shown in Table 5.1.

Table 5.3 The relative amounts of pyridine and maleic anhydride adsorption and the amounts of absorbed pyridine and maleic anhydride of acidic metal oxides

Catalyst	**Pyridine adsorption**		**Maleic anhydride adsorption**	
	Relative	**(μmole/m^2)**	**Relative**	**(μmole/m^2)**
TiO_2	1.00	0.825	1.00	6.5
$7V/TiO_2$	2.05	1.690	4.88	3.17
$8Cu7V1MgO/ TiO_2$	0.95	0.783	9.18	5.97
$8Fe7V1MgO/ TiO_2$	1.09	0.897	5.42	3.53
$8Mo7V1MgO/ TiO_2$	1.94	1.601	5.10	3.31
$8Zn7V1MgO/ TiO_2$	1.26	1.039	5.23	3.40

The research found that V_2O_5/TiO_2 catalyst was not so active for the combustion of phthalic anhydride, possibly because V_2O_5/TiO_2 catalyst had the small numbers of the adsorption sites (basic sites) and V_2O_5/TiO_2 catalyst did not have the active site or it had the small numbers of the active sites for the combustion of phthalic anhydride. Althought titania sites were active for phthalic anhydride combustion, when vanadium oxide was added into the TiO_2 support, the TiO_2 support must be covered by a complete monolayer of the surface vanadia species (>2% V_2O_5/TiO_2) with the strong interaction between vanadia and the TiO_2 surface. The surface vanadia species were active for the oxidation of o-xylene to phthalic anhydride than the combustion of phthalic anhydride.

When loading both transition metal oxide and magnesium oxide into V_2O_5/TiO_2 catalyst, it was found that metal-V-Mg-O/TiO_2 catalysts give the phthalic anhydride combustion higher than V_2O_5/TiO_2 catalyst, indicating that the transition metals were able to catalyze the reaction. Because the addition of the transition metal oxides to

V_2O_5/TiO_2 catalyst would increase the active sites on the surface of catalyst. Moreover, the increment of the maleic anhydride adsorption indicated that the addition of magnesium oxide would increase the numbers of the basic sites on surface of V_2O_5/TiO_2 catalyst and increased the adsorption of phthalic anhydride, thus, provided more opportunity to react with metal, resulting in higher activity[Charoenruay (2003)].

5.3 Catalytic reaction

This research investigated effect of hexane on phthalic anhydride combustion over V_2O_5 catalyst impregnated with transition metal oxide (Cu, Fe, Mo and Zn) and magnesium oxide. The reactions in this experiment were divided into 2 parts. First, the reactions of phthalic anhydride and hexane are individually studied. Next mixture of phthalic anhydride and hexane were investigated.

5.3.1 Combustion of phthalic anhydride.

Phthalic anhydride comprises of an anhydride functional group and a benzene ring. It was a product in the oxidation of o-xylene This reaction was studied in an excess oxygen atmosphere. The combustion reaction was as follows:

$$C_8H_4O_3 + 7.5\ O_2 \longrightarrow 8\ CO_2 + 2\ H_2O$$

In previous work, it was found that magnesium oxide could promote the adsorption of phthalic anhydride leading to better combustion of phthalic anhydride [Tongsang (2001) and Umpo (2001)]. The subsequent study found that the ratio of transition metal oxide per magnesium oxide should be at an appropriate ratio to keep a balance between the adsorption of the phthalic anhydride and the catalytic activity of the transition metal oxides [Nuampituk (2002) and Nugoolchit (2002)]. The catalytic combustion of phthalic anhydride showed in figure 5.2 to figure 5.5 [Charoenruay (2003)].

5.3.2 Combustion of Hexane.

Hexane is a member of the alkane or paraffin series of hydrocarbon. Hexane is used in low temperature thermometer, polymerization reaction, plant diluents, alcohol denaturant and solvents for vegetable oils. This reaction was studied in an excess oxygen atmosphere. The combustion reaction of hexane was as follows:

$$C_6H_{14} + 9.5\ O_2 \longrightarrow 6\ CO_2 + 7\ H_2O$$

The results obtained from the catalytic combustion of hexane showed in figure 5.2 to figure 5.5.

Figure 5.6 illustrate the catalytic activity of 8Cu7V1Mg/TiO_2 for hexane combustion. For 8Cu7V1Mg/TiO_2 catalyst, the conversion of hexane rapidly increased from 8 to 75% at temperature range of 200 to 300°C and steadily increased to 97% at 500°C.

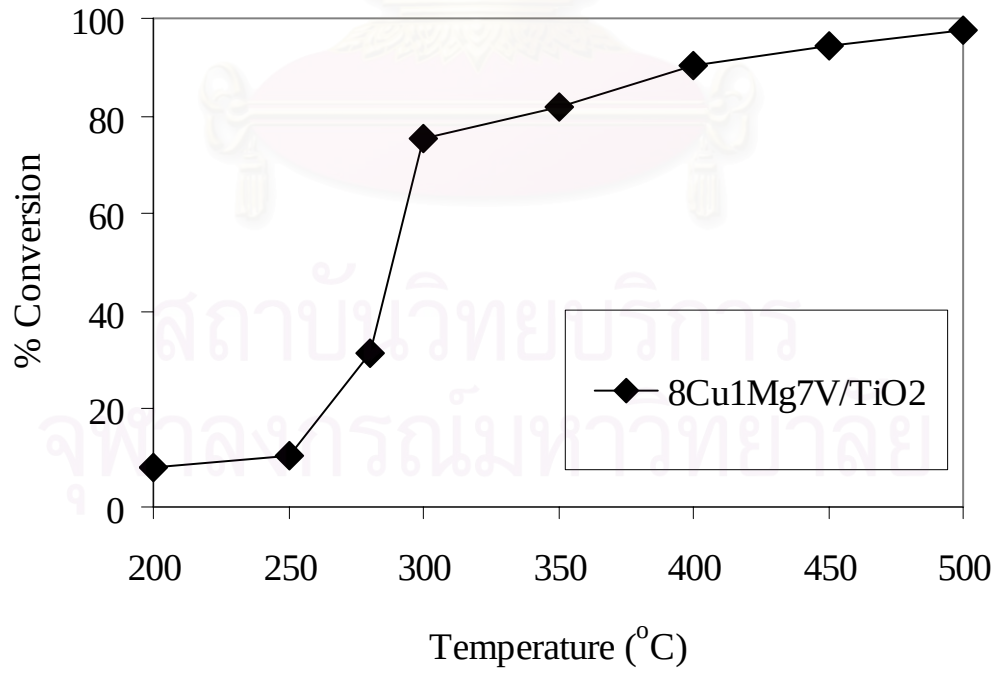

Figure 5.2 The catalytic activity of copper oxide catalyst for the combustion of hexane.

Figure 5.3 show the catalytic activity of 8Fe7V1Mg/TiO_2 for the combustion of phthalic anhydride. It was found that 8Fe7V1Mg/TiO_2 catalyst exhibited the phthalic anhydride conversion as about 1 to 60% in the range of temperature 200 to 300°C and steadily increased until the temperature reached 500°C, which the conversion was about 92%.

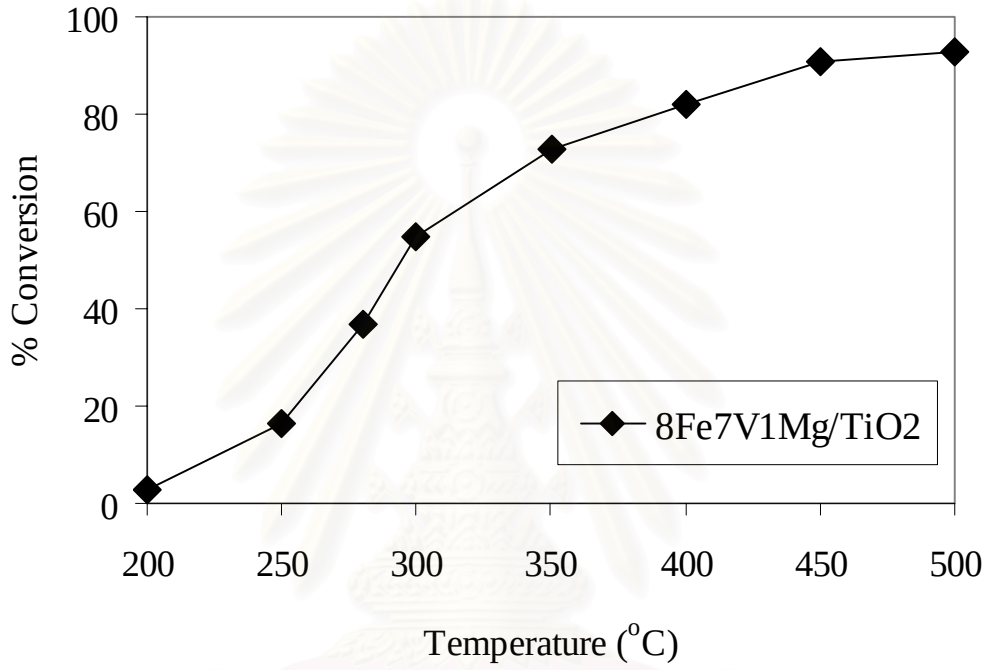

Figure 5.3 The catalytic activity of iron oxide catalyst for the combustion of phthalic anhydride.

Figure 5.4 show the catalytic activity of 8Mo7V1Mg/TiO_2 for the combustion of phthalic anhydride. It was found that the conversion of phthalic anhydride steadily increased from 5 to 95% at temperature range of 200 to 500°C for 8Mo7V1Mg/TiO_2 catalyst.

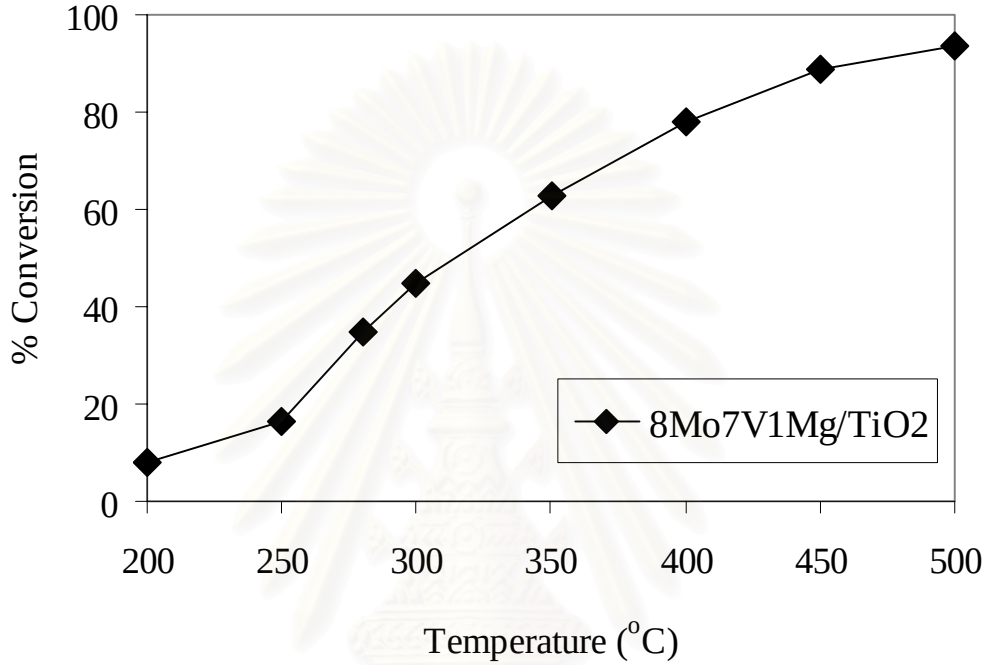

Figure 5.4 The catalytic activity of molybdenum oxide catalyst for the combustion of phthalic anhydride.

Figure 5.5 shown the catalytic activity of 8Zn7V1Mg/TiO_2 for the combustion of phthalic anhydride. It was found that the conversion of phthalic anhydride on 8Zn7V1Mg/TiO_2 catalyst rapidly increased from 3 to 70% at the temperature range of 200 to 300°C. After that it steadily increased until the temperature reached 500°C, which the conversion was about 90%.

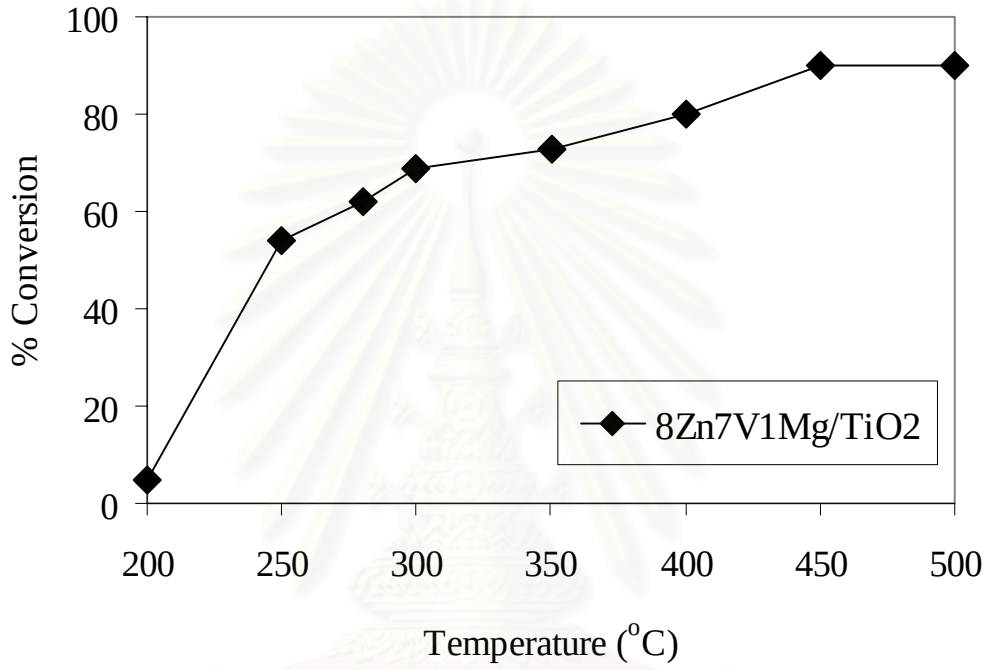

Figure 5.5 The catalytic activity of zinc oxide catalyst for the combustion of phthalic anhydride.

5.3.3 Combustion of phthalic anhydride in the presence of hexane

This part reports that the combustion of phthalic anhydride and hexane (co-feeding). Figure 5.10 to figure 5.15 showed catalytic activity of the catalysts for the combustion of phthatic anhydride in mixture compared the catalytic activity of catalyst for the combustion of phthatic anhydride pure component.

- **Copper oxide catalyst**

Figure 5.10 illustrates the catalytic activity of 8Cu7V1Mg/TiO_2 for phthalic anhydride combustion with hexane co-feeding. The result showed that the activity of phthalic anhydride was slightly different from the combustion of phthalic anhydride in pure component. Figure 5.11 illustrates the catalytic activity of 8Cu7V1Mg/TiO_2 for hexane combustion in the reaction. , In gas mixture, a result showed a decrease in hexane conversion at the same temperature compared with combustion of hexane in pure component. It would probably due to the effect of competitive adsorption of the reactants. The added hexane did not affect phthalic anhydride combustion but the conversion of hexane was retarded. It may be implied that the combustion of phthalic anhydride and hexane used the same active sites. From results of pyridine and maleic anhydride adsorption, 8Cu7V1Mg/TiO_2 catalyst had small numbers of the actives sites and the large number of basic sites. The large number of basic sites implies large amount of phthalic anhydride adsorption which enhance combustion of phthalic anhydride.

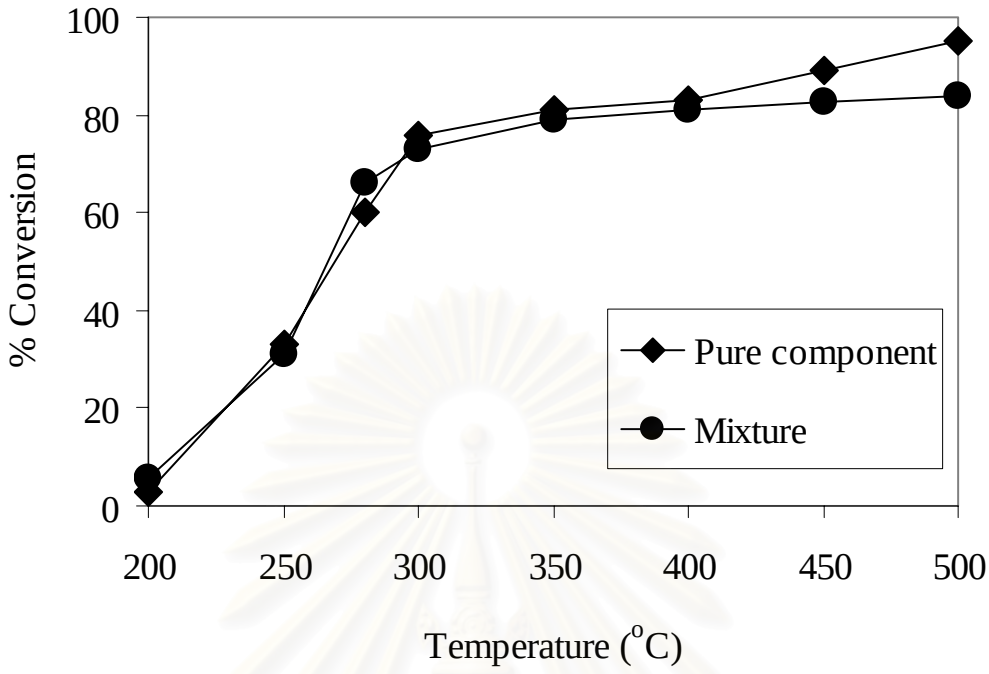

Figure 5.6 The catalytic activity of copper oxide catalyst for the combustion of phthalic anhydride.

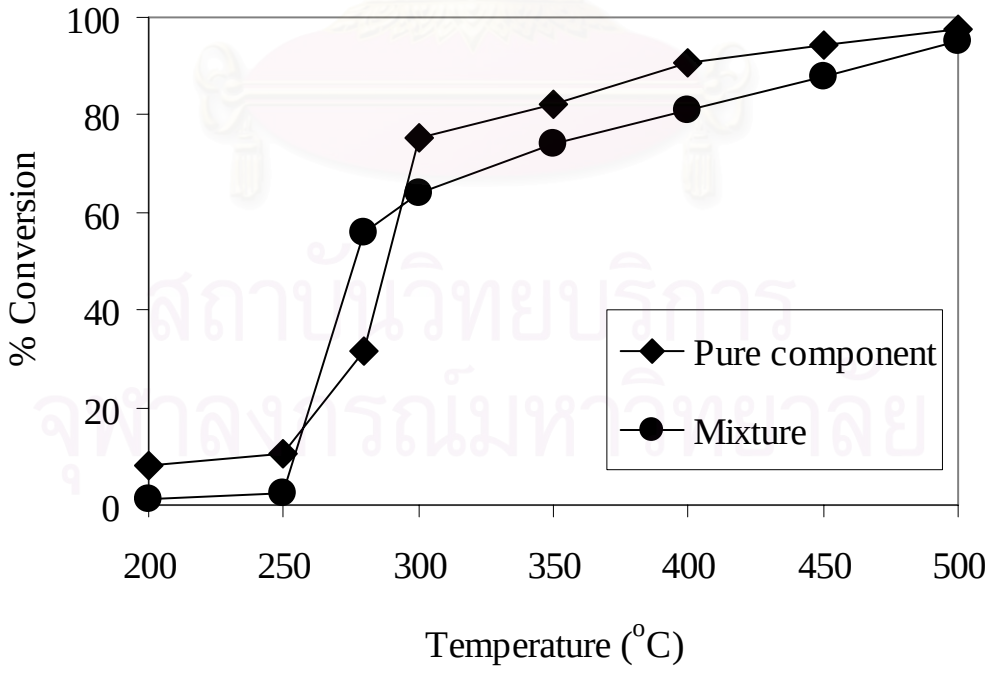

Figure 5.7 The catalytic activity of copper oxide catalyst for the combustion of hexane.

- **Iron oxide catalysts**

Figure 5.12 illustrates the catalytic activity of 8Fe7V1Mg/TiO_2 for phthalic anhydride combustion with hexane co-feeding. The result obtained from the combustion of phthalic anhydride alone is shown here for comparison. Figure 5.13 illustrates the catalytic activity of 8Fe7V1Mg/TiO_2 for hexane combustion in the reaction. In the gas mixture, the decrease of hexane conversion at the same temperature compared with combustion of hexane in pure component was obsered. The mutual effect of hexane and phthalic anhydride light-off suggests the involvement of intermediate(s) from hexane or phthalic anhydride partial oxidation.

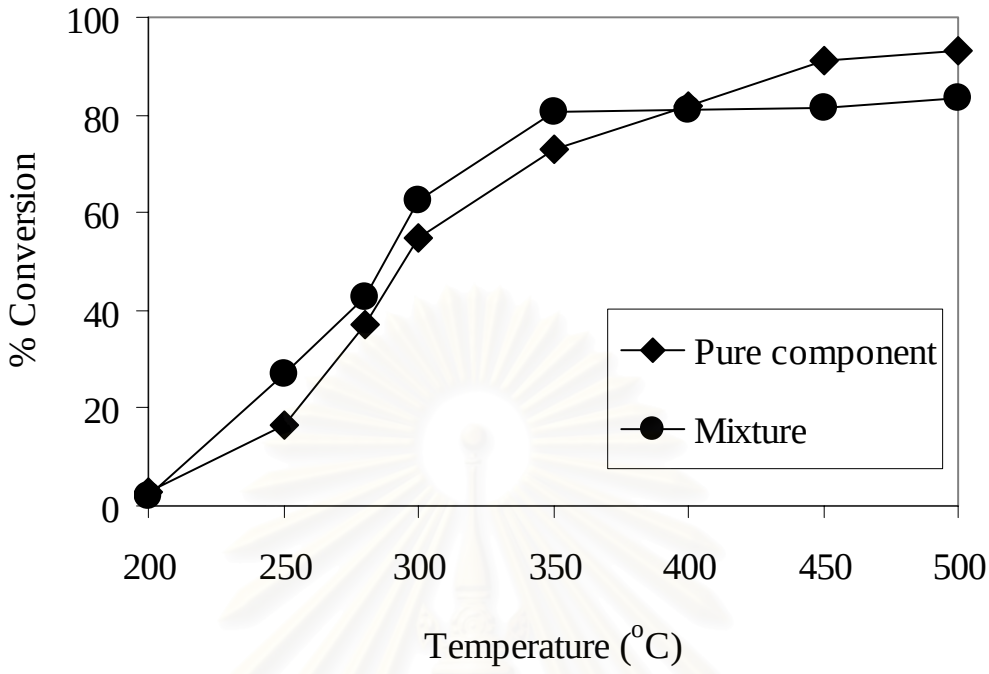

Figure 5.8 The catalytic activity of iron oxide catalyst for the combustion of phthalic anhydride.

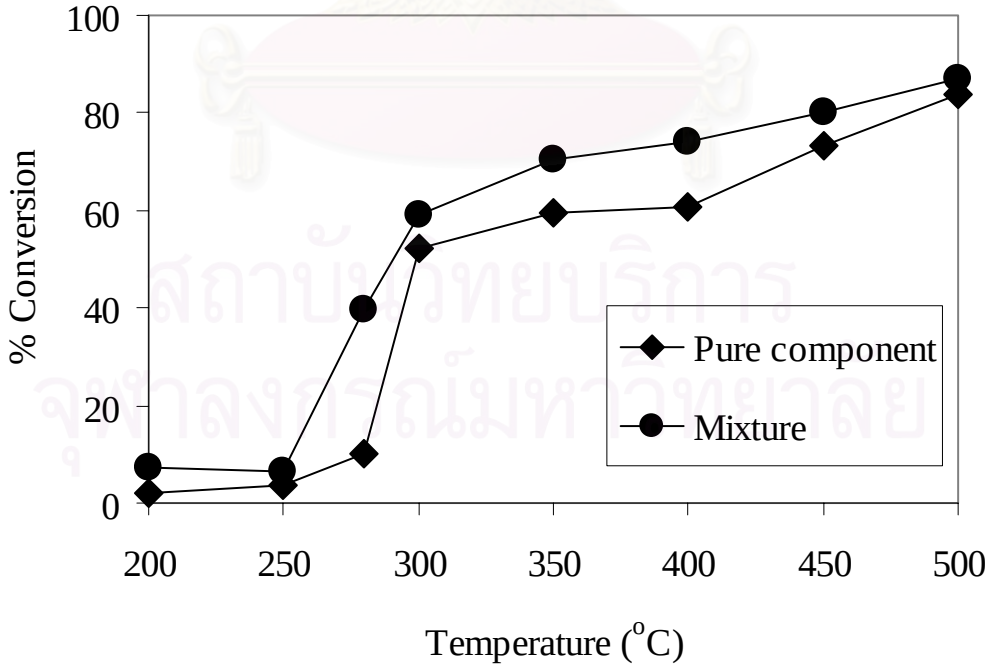

Figure 5.9 The catalytic activity of iron oxide catalyst for the combustion of hexane.

- **Molybdenum oxide catalysts**

Figure 5.14 illustrates the catalytic activity of 8Mo7V1Mg/TiO_2 for phthalic anhydride combustion with hexane co-feeding. The result showed that when hexane was co-feed with phthalic anhydride, the conversion of slightly decreased. Figure 5.15 illustrates the catalytic activity of 8Mo7V1Mg/TiO_2 for hexane combustion in the mixture. In the gas mixture, the decrease of hexane and phthalic anhydride conversion was observed. It would probably be the effect of competitive adsorption of reactant. Hence, no one species was able to dominate the adsorption on the active sites and thereby completely prevented the adsorption and reaction of other species.

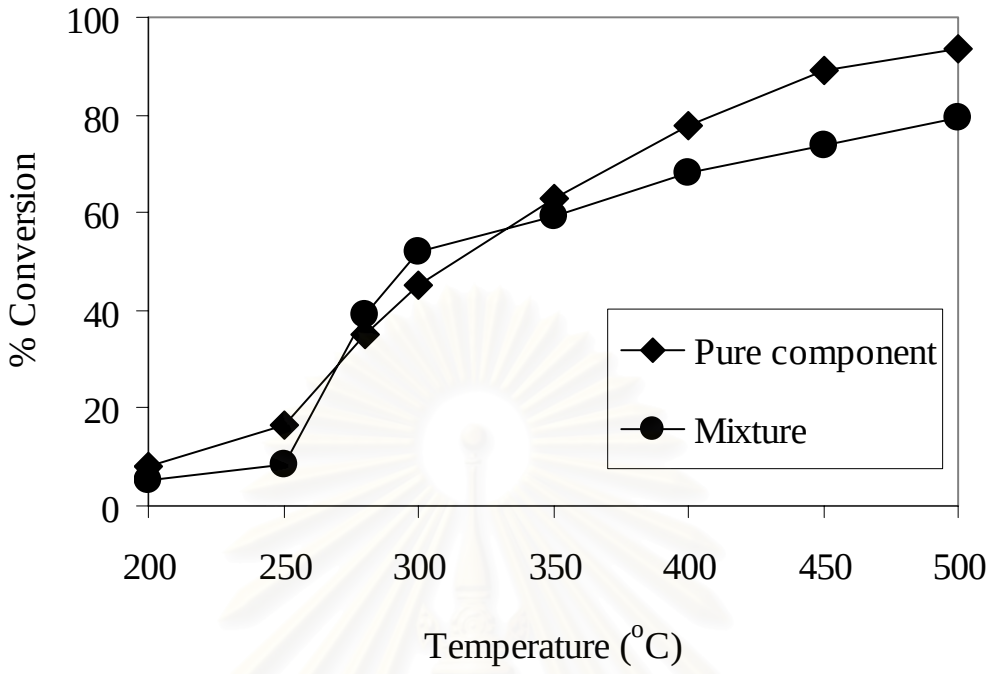

Figure 5.10 The catalytic activity of molybdenum oxide catalyst for the combustion of phthalic anhydride.

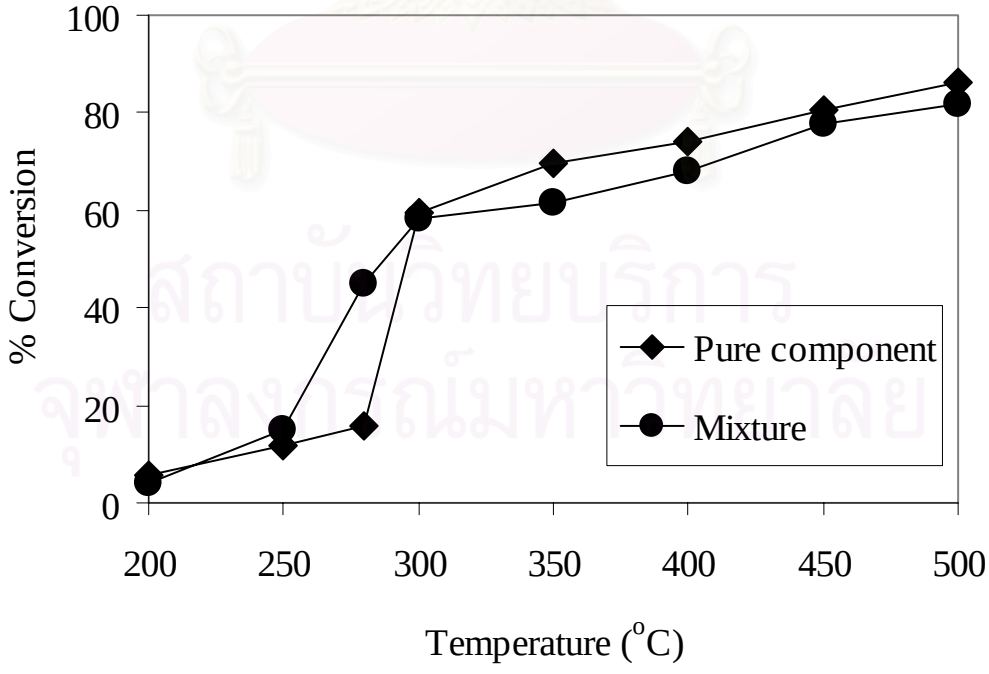

Figure 5.11 The catalytic activity of molybdenum oxide catalyst for the combustion of hexane.

- **Zinc oxide catalysts**

Figure 5.16 illustrates the catalytic activity of 8Zn7V1Mg/TiO_2 for phthalic anhydride combustion with hexane co-feeding. The result showed that when hexane was co-feed with phthalic anhydride, the conversion of slightly decreased. Figure 5.17 illustrates the catalytic activity of 8Zn7V1Mg/TiO_2 for phthalic anhydride combustion with hexane co-feeding. The result showed that the conversion was slightly of hexane had little different from the combustion of hexane in pure component. The addition of hexane slightly decreased the conversion of phthalic anhydride because of the competitive adsorption of the reactants on the active sites. From results of pyridine and maleic anhydride adsorption showed 8Zn7V1Mg/TiO_2 catalyst had acidity and basicity of this catalyst would be appropriate for combustion of hexane so the conversion of hexane in mixture not different from hexane conversion in pure component.

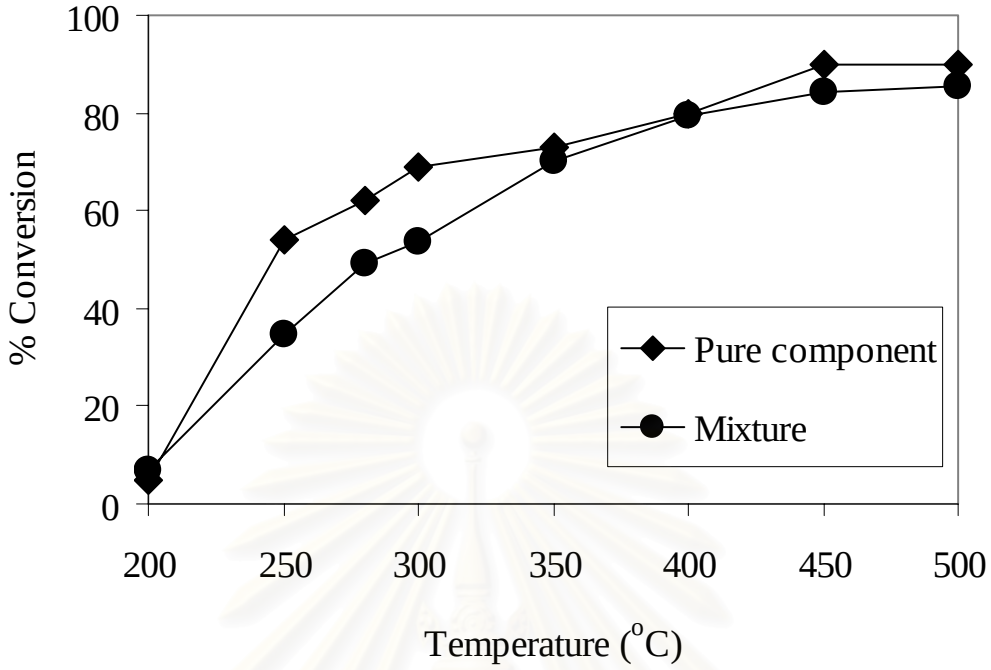

Figure 5.12 The catalytic activity of zinc oxide catalyst for the combustion of phthalic anhydride.

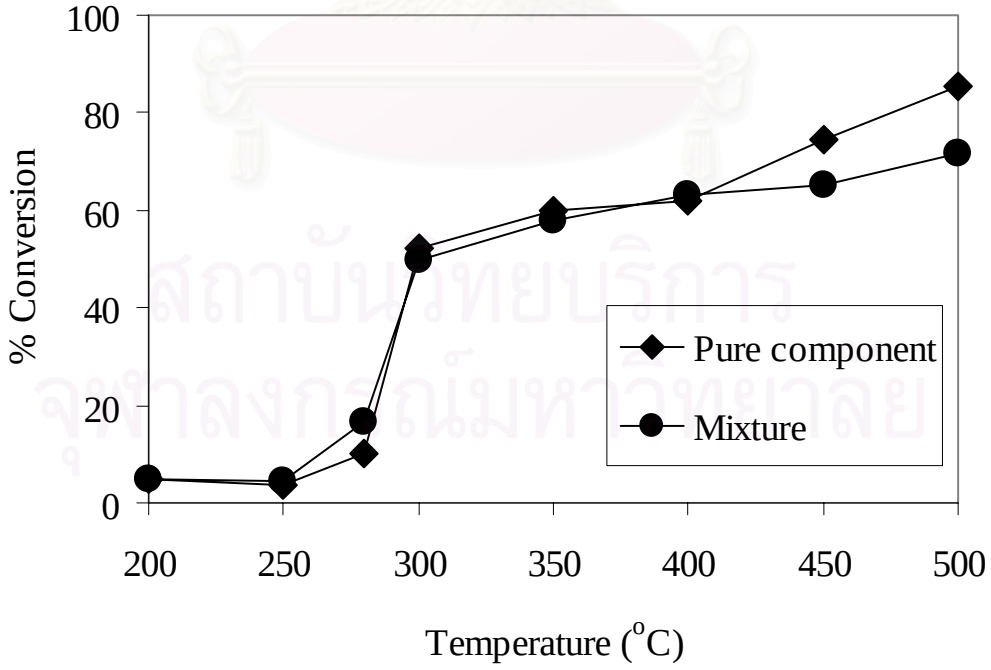

Figure 5.13 The catalytic activity of zinc oxide catalyst for the combustion of Hexane

From the result effect of addition hexane on the combustion of phthalic anhydride the results showed that there were competitive adsorption of phthalic anhydride and hexane on the catalyst. For Cu, Mo and Zn, catalysts phthalic anhydride and hexane competitively adsorbed and reacted on same active sites. Therefore, the combustion of phthalic anhydride or hexane hindranced each other depended on the adsorption ability on each catalyst. The Fe catalyst showed different result i.e. the combustion of the phthalic anhydride and hexane was promoted when both reactants were fuel together suggesting that the involvement of intermediate(s) from hexane or phthalic anhydride partial oxidation.

CHAPTER VI

CONCLUSIONS AND RECOMMENDATIONS

6.1 Conclusions

The conclusions of the present research are the following:

1. The phthalic anhydride and hexane had the same active sites for all catalysts in this experiment.

2. The adsorption sites played the role as promoter of phthalic anhydride combustion.

3. The competitive adsorption of reactants had affected the mixture combustion.

4. The mutual effect of hexane and phthalic anhydride light-off on 8Fe1Mg7V/TiO_2 suggests the involvement of intermediate(s) from hexane or phthalic anhydride partial oxidation

5. The addition of hexane had possibility to improve phthalic anhydride combustion.

6.2 Recommendations for future studies

From the previous conclusions, the following recommendations for future studies can be proposed.

1. It is interesting to study the combustion of phthalic anhydride by using the other mixture such as alcohol, alkene. But one should concern about economic benefit for applications in real situation.

2. The adiabatic reactor is another interesting subject for investigating the effect of heat from addition reactants.

REFERENCES

Amiridis, M.D., Duevel, R.V., and Wachs, I.E., "The effect of metal oxide additives on the activity of V_2O_5/TiO_2 catalysts for the selective catalytic reduction of nitric oxide by ammonia", *Appl. Catal. B*, 1999, **20**, 111-122.

Anastasov, A.I., "Deactivation of an industrial V_2O_5-TiO_2 catalyst for oxidation of o-xylene into phthalic anhydride", *Chemical Engineering and Processing*, 2003, **42**, 449-460.

Anderson, J.R., and Pratt, K.C., *Introduction to characterization and testing of catalyst*, Sydney: Academic Press, 1985.

Brink, R.W., Mulder, P., and Louw, R., "Catalytic combustion of chlorobenzene on Pt/γ-Al2O3 in the presence of aliphatic hydrocarbons" *Catalysis Today*, 1999, **54**, 101–106.

Brink, R.W., Mulder, P., and Louw, R, "Increased combustion rate of chlorobenzene on Pt/γ-Al2O3 in binary mixtures with hydrocarbons and with carbon monoxide", *Catalysis Today*, 2000, **25**, 229-237.

Bond, G. C., *Heterogeneous Catalysis principles and applications: Chemisorption at oxide surfaces*, Oxford: Clarendon Press, 1987.

Busca, G., Daturi, M., Finocchio, E., Lorenzelli, V., Ramis, G., and Willey, R.J., "Transition metal mixed oxides as combustion catalysts: preparation, characterization and activity mechanisms", *Catalysis Today*, 1997, **33**, 239-249.

Centeno, M.A., Paulis, M., Montes, M., and Odriozola, J.A., "Catalytic combustion of volatile organic compounds on $Au/CeO_2/Al_2O_3$ and Au/Al_2O_3 catalysts", *Appl. Catal. A*, 2002, **234**, 65-78.

Chaiyasit, N., "Application of the Co-Mg-O/TiO_2 catalyst on the selective oxidation of alcohols", *Master's Thesis, Faculty of Engineering, Chulalongkorn University*, 2000.

Cimino, S., Di Benedetto, A., Pirone, R., and Russo, G., "CO, H_2 or C_3H_8 assisted catalytic combustion of methane over supported $LaMnO_3$ monoliths", *Catalysis Today*, 2003, **83,** 33–43.

Deutschmann, O., Maier, L.I., Riedel, U., Stroemman, A.H., and Dibble, R.W., "Hydrogen assisted catalytic combustion of methane on platinum", *Catalysis Today*, 2000, **59,** 141–150.

Dias, C.R., Portela M.F., and Bond G.C., "Oxidation of o-xylene to phthalic anhydride over V_2O_5/TiO_2 catalysts", *Journal of Catalysis*, 1995, **157**, 353-358.

Dias, C.R., Portela, M.F., Bañares, M.A., Galán-Fereres, M., López-Granados, M., Peña, M.A., and Fierro, J.L.G., "Selective oxidation of *o*-xylene over ternary V-Ti-Si catalysts", *Appl. Catal. A.*, 2002, **224,** 141–151.

Gangwal, S.K., Mullins, M.E., Spivey, J.J., and Caffrey, P.R., "Kinetics and selectivivity of deep catalytic", *Appl. Catal.*, 1988, **36**, 231-247.

Gervasini A., Pirola C., and Ragaini V., "Destruction of carbon tetrachloride in the presence of hydrogen-supplying compounds with ionization and catalytic oxidation", *Appl Catal B*, 2002, **38**, 17–28.

Graham, J.L., Almquist, C.B., Kumarb, S., and Sidhu, S.,"An investigation of nanostructured vanadia/titania catalysts for the oxidation of monochlorobenzene", *Catalysis Today*, 2003, **88,** 73–82.

Hayes N.W., Richard W. Joyner R.W., and Efim S. Shpiro E.S.,"Infrared spectroscopy studies of the mechanism of the selective reduction of NO, over Cu ZSM-5 catalysts *Appl Catal B*, 1996, **8**, 343-363.

Hess, K., Morsbach, B., Drews, R., Buechele, W., and Schachner, H., "Catalyst containing metal oxides for use in the degenerative oxidation of organic compounds present in exhaust gases from combustion plants", *United States Patent*, 1993, **5227356**, 1-20.

Kang, Y.M., and Wan, B.Z., "Effects of acid or base additives on the catalytic combustion activity of chromium and cobalt oxide", *Appl. Catal. A*, 1994, **114**, 35-49.

Keuneche, G., Klopfer, A., and Sterck, L., "Process for continuously separating phthalic anhydride from the reaction gases of the catalytic oxidation of o-xylene and/or naphthalene", *United States Patent*, 1981, **4285871**, 1-22.

Kim, S.C., "The catalytic oxidation of aromatic hydrocarbons over supported metal oxide", *Journal of Hazardous Materials*, 2002, **B91**, 285-299.

Kirk-Othmer. *Encyclopedia of chemical technology: Acidic and Basic catalysts*, John wiley&Sons Inc., 1979.

Larsson, P.-O., Berggren, H., Andersson, A., and Augustsson, O.,"Supported metal oxides for catalytic combustion of CO and VOCs emissions: preparation of titania overlayers on a macroporous support", *Catalysis Today*, 1997, **35**, 137-144.

Leklertsunthorn, R., "Oxidation property of the V-Mg-O/TiO_2 catalyst", *Master's Thesis, Department of Engineering, Graduate School, Chulalongkorn University*, 1998.

Lietti, L., Nova, I., Ramis, G., Dall'Acqua, L., Busca, G., Giamello, E., Forzatti, P., and Bregani, F., "Characterization and reactivity of V_2O_5-MoO_3/TiO_2 De-NO_x SCR catalysts", *Journal of Catalysis*, 1999, **187**, 419-435.

López-Fonseca, R., Gutiérrez-Ortiz, J.I., Ayastui, J.L., Gutiérrez-Ortiz, M.A., and González-Velasco, J.R.,"Gas-phase catalytic combustion of chlorinated VOC binary mixtures", *Appl. Catal. B.* 2003, **45,** 13–21.

Minicò, S., Scirè, S., Crisafulli, C., Maggiore, R., and Galvagno, S., "Catalytic combustion of volatile organic compounds on gold/iron oxide catalysts", Appl. Catal. B., 2000, **28,** 245–251.

Mongkhonsi, T., and Kershenbaum, L., "The effect of deactivation of a V_2O_5/TiO_2 (anatase) industrial catalyst on reactor behaviour during the partial oxidation of o-xylene to phthalic anhydride", *Appl. Catal. A*, 1998, **170**, 33-48.

Nuampituk, S., "Effect of transition metal and magnesium loading sequence on the combustion of phthalic anhydride over MgO promoted transition metal oxide catalysts", *Master's Thesis, Faculty of Engineering, Chulalongkorn University*, 2002.

Nugoolchit, J., "Effect of MgO on the combustion of phthalic anhydride over transition metal oxide catalysts", *Master's Thesis, Faculty of Engineering, Chulalongkorn University*, 2002.

Ordóñez, S., Bello, L., Sastre, H., Rosal, R., and D´ýez, F.V.,"Kinetics of the deep oxidation of benzene, toluene, *n*-hexane and their binary mixtures over a platinum on γ-alumina catalyst", *Appl. Catal. B.*, 2002, **38,** 139–149.

Ozkan, U.S., Harris, T.A., and Schilf, B.T., "The partial oxidation of C 5 hydrocarbons over vanadia-based catalysts", *Catalysis Today*, 1997, **33**, 57-71.

O'Malley, A., and Hodnett, B.K., "The influence of volatile organic compound structure on conditions required for total oxidation", *Catalysis Today*, 1999, **54**, 31–38

Perry, R.H., and Chilton, C.H., *Chemical Engineering Handbook*, 1973.

Reid, R.C., Pranusnitz, J.M., and Poling, B.E., *The Properties of Gases and Liquids*, McGraw-Hill International Book Company, 1988.

Satterfield, C. N., *Heterogeneous Catalysis in Industrial Practice: Heterogeneous Catalytic Oxidation*, McGraw-Hill, 1980.

Spivey, J.J., "Complete Oxidation of Volatile Organics", *Ind. Eng. Chem.Res*., 1987, **26**, 2165-2180.

Thammanokul, H., "Oxidative dehydrogenation of propane over V-Mg-O catalysts", *Master's Thesis, Faculty of Engineering, Chulalongkorn University*, 1996.

The JCPDS., *Inorganic Phases Alphabetical Index*, 1980.

Tongsang, P., "The application of V-Mg-O/TiO_2 catalyst on the combustion of anhydrides", *Master's Thesis, Faculty of Engineering, Chulalongkorn University*, 2001.

Toyada, Y., and Teraji, S., "Process for the treatment of byproducts obtained in the preparation of phthalic anhydride", *United States Patent*, 1980, **4181489**, 1-18.

Umpo, S., "The application of Co-Mg-O/Al_2O_3 catalyst on the combustion of anhydrides", *Master's Thesis, Faculty of Engineering, Chulalongkorn University*, 2001.

Way, T., and Peter, F., "Apparatus for the recovery of vaporized phthalic anhydride from gas streams" *United States Patent*, 1981, **4252772**, 1-20.

APPENDICES

APPENDIX A
CALCULATION OF CATALYST PREPARATION

Preparation of 8Cu-7V-1Mg-O/ TiO_2 catalysts by the Wet Impregnation Method is shown as follow:

Reagent: - Cupric nitrate trihydrate($CuN_2O_6 \cdot 3H_2O$)
Molecular weight = 241.60 g.
- Magnesium nitrate [$Mg(NO_3)_2$]
Molecular weight = 256.41 g.
- Ammonium metavanadate [$NH_4(VO_3)$]
Molecular weight = 116.98 g

Support - Titania [TiO_2]

Calculation for the preparation of the 8Cu-7V_2O_5-1Mg-O/TiO_2 catalyst.

The 8Cu-7V_2O_5-1Mg-O/TiO_2 aqueous solution used in catalyst preparation consists of V_2O_5 7wt% and TiO_2 93wt%. The amounts of copper and magnesium in 8Cu-7V_2O_5 -1Mg-O/ TiO_2 catalyst are calculated as follows:

Preparation of :7V_2O_5/TiO_2 5 g
If the weight of catalyst was 100 g, 7V_2O_5/TiO_2 would compose of V_2O_5 7 g and TiO_2 93 g. Therefore, in this system,

the amount of V_2O_5 = 7/100 × 5
= 0.35 g

Vanadia (V_2O_5) 0.35 g was prepared from $NH_4(VO_3)$ and molecular weight of V_2O_5 = 181.88 , then

the amount of content $NH_4(VO_3)$ used
= (116.98/181.88)×0.35
= 0.4502 g

Thus

The amount of TiO_2 = 5-0.35

= 4.65 g

basis :$7V_2O_5/TiO_2$ 5 g

Then, the Cu: (support + V_2O_5) weight ratio = 8:92

The amount of Cu = $8/92 \times 5$

= 0.4348 g

Copper (Cu) 0.4348 g was impregnated from ($CuN_2O_6{\cdot}3H_2O$) solution and molecular weight of Cu = 63.546 g

the amount of ($CuN_2O_6{\cdot}3H_2O$) used = $(0.4348\times241.60)/(63.546)$

= 1.6531 g

and the Mg: ($7V_2O_5/TiO_2$ + Cu) weight ratio = 1:100

The amount of Mg = $(5+0.4348)\times1/100$

= 0.0543 g

Magnesium (Mg) 0.0543 g was impregnated from $Mg(NO_3)_2$ solution 99% and molecular weight of Mg = 24.305 g

Thus, the amount of $Mg(NO_3)_2$ used = $(0.0543\times256.41\times100)/(24.305\times99)$

= 0.5791 g

The calculation for the preparation of other catalysts as follow 8Fe-$7V_2O_5$-1Mg-O/ TiO_2, 8Mo-$7V_2O_5$-1Mg-O/ TiO_2 and 8Zn-$7V_2O_5$-1Mg-O/ TiO_2 catalysts were the same as the preparation of 8Cu-$7V_2O_5$-1Mg-O/ TiO_2 catalysts.

APPENDIX B

CALCULATION OF DIFFUSIONAL LIMITATION EFFECT

In the present work there are doubt whether the external and internal diffusion limitations interfere with the phthalic anhydride and hexane combustion reaction. Hence, the kinetic parameters were calculated based on the experimental data so as to prove the controlled system. The calculation is divided into two parts; one of which is the external diffusion limitation, and the other is the internal diffusion limitation.

1. External diffusion limitation

The phthalic anhydride and hexane combustion reaction is considered to be an irreversible first order reaction occurred on the interior pore surface of catalyst particles in a fixed bed reactor. Assume isothermal operation for the reaction.

In the experiment, 0.01% phthalic anhydride, 0.24% hexane and 21% O_2 was used as reactant in the system. Because percentage of phthalic anhydride and hexane was rather small compared to the oxygen there were can be neglected. Molecular weight of nitrogen and oxygen are 28.02 and 31.98, respectively. Thus, the average molecular weight of the gas mixture was calculated as follows:

$$M_{AB} = 0.79\times28.02 + 0.21\times31.98$$
$$= 28.85 \text{ g/mol}$$

Calculation of reactant gas density

Consider the phthalic anhydride combustion is operated at low pressure and high temperature(500°C). We assume that the gases are respect to ideal gas law. The density (ρ) of such gas mixture reactant at various temperatures (T) is calculated in the following.

$$\rho = PM / RT$$

where ρ = gas density

M = molecular weight

R = gas constant

T = absolute temperature

We obtained : $\rho = 0.455$ kg/m^3

Calculation of the gas mixture viscosity

The simplified methods for determining the viscosity of low pressure binary are described elsewhere (Reid, 1988). The method of Wilke is chosen to estimate the gas mixture viscosity.

For a binary system of 1 and 2,

$$\mu_m = \frac{y_1\mu_1}{y_1 + y_2\Phi_{12}} + \frac{y_2\mu_2}{y_2 + y_1\Phi_{21}}$$

where μ_m = viscosity of the mixture

μ_1, μ_2 = pure component viscosity

y_1 , y_2 = mole fractions

$$\phi_{12} = \frac{\left[1+\left(\frac{\mu_1}{\mu_2}\right)^{1/2}\left(\frac{M_1}{M_2}\right)^{1/4}\right]^2}{\left[8\left(1+\frac{M_1}{M_2}\right)\right]^{1/2}}$$

$$\phi_{21} = \phi_{12}\left(\frac{\mu_2}{\mu_1}\right)\left(\frac{M_1}{M_2}\right)$$

M_1, M_2 = molecular weight

Let 1 refer to nitrogen and 2 to oxygen

$M_1 = 28.02$ and $M_2 = 31.98$

From Perry(1973) the viscosity of nitrogen at 500°C are 0.0368 cP. The viscosity of oxygen at 500°C are 0.039cP.

$\phi_{12} = 0.971$

$\phi_{21} = 0.902$

$\mu_m = 3.81 \times 10^{-5}$ kg/m-s

Calculation of diffusion coefficients

Diffusion coefficients for binary gas system at low pressure calculated by empirical correlation are proposed by Reid (1988). Wilke and Lee method is chosen to estimate the value of D_{AB} due to the general and reliable method. The empirical correlation is

$$D_{AB} = \frac{\left(3.03 - \frac{0.98}{M_{AB}^{1/2}}\right)(10^{-3})T^{3/2}}{PM_{AB}^{1/2}\sigma_{AB}^2\Omega_D}$$

where D_{AB} = binary diffusion coefficient,cm^2/s

T = temperature,K

M_A ,M_B = molecular weights of A and B ,g/mol

$$M_{AB} = 2\left[\left(\frac{1}{M_A}\right) + \left(\frac{1}{M_B}\right)\right]^{-1}$$

P = pressure,bar

σ = characteristic length,^{0}A

Ω_D = diffusion collision integral, dimensionless

The characteristic Lennard-Jones energy and Length, ε and σ , of nitrogen and oxygen are as follows: (Reid,1988)

For O_2 : σ = 3.467 ^{0}A, ε/k = 106.7

For N_2 : σ = 3.798 ^{0}A , ε/k = 71.4

The sample rules are usually employed.

$$\sigma_{AB} = \frac{\sigma_A + \sigma_B}{2} = \frac{3.798 + 3.467}{2} = 3.63$$

$$\varepsilon_{AB}/k = \left(\frac{\varepsilon_A \varepsilon_B}{k^2} \right)^{1/2} = (71.4 \times 106.7)^{1/2} = 87.28$$

Ω_D is tabulated as a function of kT/ε for the Lennard-Jones potential. The accurate relation is

$$\Omega_D = \frac{A}{(T^*)^B} + \frac{C}{\exp(DT^*)} + \frac{E}{\exp(FT^*)} + \frac{G}{\exp(HT^*)}$$

where $T^* = \frac{kT}{\varepsilon_{AB}}$, A = 1.06036 , B = 0.15610 , C = 0.19300 , D = 0.47635 , E = 1.03587 , F = 1.52996 , G = 1.76474 , H = 3.89411

Then T^* = 8.857

$$\Omega_D = \frac{1.06036}{(T^*)^{0.15610}} + \frac{0.19300}{\exp(0.47635T^*)} + \frac{1.03587}{\exp(1.52996T^*)} + \frac{1.76474}{\exp(3.89411T^*)}$$

Ω_D = 0.757

With Equation of D_{AB},

$D(N_2\text{-}O_2)$ = 1.123 m^2/s

Reactant gas mixture was supplied at 100 ml/min. in tubular microreactor used in the phthalic anhydride oxidation system at 30°C

air flow rate through reactor = 100 ml/min. at 30°C

The density of air , ρ = 1.161 kg/m^3

Mass flow rate = 1.935×10^{-6} kg/s

Diameter of stainless steel tube reactor = 9.5 mm

Cross-sectional area of tube reactor = $\frac{\pi(9.5\times10^{-3})^2}{4}$ = 7.09×10^{-5} m^2

Mass Velocity , G = 0.027 kg/m^2-s

Catalyst size = 40-60 mesh = 0.178-0.126 mm

Average catalyst size = (0.126+0.178)/2 = 0.152 mm

Find Reynolds number, Re_p, which is well known as follows:

$$Re_p = \frac{d_p G}{\mu}$$

We obtained

$$Re_p = 0.108$$

Average transport coefficient between the bulk stream and particles surface could be correlated in terms of dimensionless groups, which characterize the flow conditions. For mass transfer the Sherwood number, $k_m\rho/G$, is an empirical function of the Reynolds number, d_pG/μ, and the Schmit number, $\mu/\rho D$. The j-factors are defined as the following functions of the Schmidt number and Sherwood numbers:

$$j_D = \frac{k_m \rho}{G}\left(\frac{a_m}{a_t}\right)(\mu/\rho D)^{2/3}$$

The ratio (a_m/a_t) allows for the possibility that the effective mass-transfer area a_m, may be less than the total external area, a_t, of the particles. For Reynolds number greater than 10, the following relationship between j_D and the Reynolds number well represents available data.

$$j_D = \frac{0.458}{\varepsilon_B}\left(\frac{d_p G}{\mu}\right)^{-0.407}$$

where G = mass velocity(superficial) based upon cross-sectional area of empty reactor

(G = uρ)

d_p = diameter of catalyst particle for spheres

μ = viscosity of fluid

ρ = density of fluid

ε_B = void fraction of the interparticle space (void fraction of the bed)

D = molecular diffusivity of component being transferred

Assume $\varepsilon_B = 0.5$

$j_D = 2.266$

A variation of the fixed bed reactor is an assembly of screens or gauze of catalytic solid over which the reacting fluid flows. Data on mass transfer from single screens has been reported by Gay and Maughan. Their correlation is of the form

$$j_D = (\varepsilon k_m \rho/G)(\mu/\rho D)^{2/3}$$

Where ε is the porosity of the single screen.

Hence, $k_m = (j_D G/\rho)(\mu/\rho D)^{-2/3}$

$$k_m = \left(\frac{0.458G}{\varepsilon_B \rho}\right) Re^{-0.407}\, Sc^{-2/3}$$

Find Schmidt number, Sc : $Sc = \frac{\mu}{\rho D}$

$Sc = 7.456 \times 10^{-5}$

Find k_m : $k_m = 75.90$ m/s

Properties of catalyst

Density = 0.375 g/ml catalyst

Diameter of 40-60 mesh catalyst particle = 0.152 mm

Weight per catalyst particle = $\frac{\pi(0.152\times10^{-1})^3\times0.375}{6} = 6.895\times10^{-7}$ g/particle

External surface area per particle = $\pi(0.152\times10^{-3})^2 = 7.26\times10^{-8}$ m^2/particle

$a_m = (7.26\times10^{-8})/(6.895\times10^{-7}) = 0.105$ m^2/gram catalyst

Volumetric flow rate of gaseous feed stream = 100 ml/min

Molar flow rate of gaseous feed stream = 6.71×10^{-5} mol/s

Hexane molar feed rate = $0.0024\times6.71\times10^{-5} = 1.61\times10^{-7}$ mol/s

Hexane conversion (experimental data): 97.53% at 500°C

The estimated rate of phthalic anhydride oxidation reaction is based on the ideal plug flow reactor which there is no mixing in the direction of flow and complete mixing perpendicular to the direction of flow (i.e., in the radial direction). The rate of reaction will vary with reaction length. Plug flow reactors are normally operated at steady state so that properties at any position are constant with respect to time. The mass balance around plug flow reactor becomes

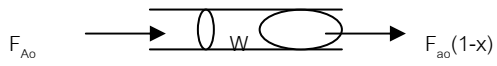

$\{\text{rate of i into volume element}\} - \{\text{rate of i out of volume element}\}$

$+ \{\text{rate of production of i within the volume element}\}$

$= \{\text{rate of accumulation of i within the volume elecment}\}$

$$F_{Ao} = F_{Ao}(1-x) + (r_W W)$$
$$(r_W W) = F_{Ao} - F_{Ao}(1-x) = F_{Ao} = F_{Ao}x$$

$$r_W = \frac{F_{Ao}x}{W} = 1.57 \times 10^{-6} \text{ mol/s-gram catalyst}$$

At steady state the external transport rate may be written in terms of the diffusion rate from the bulk gas to the surface. The expression is:

$$R_{obs} = k_m a_m (C_b - C_s)$$
$$= \frac{\text{phthalic anhydride converted (mole)}}{\text{(time)(gram of catalyst)}}$$

where C_b and C_s are the concentrations in the bulk gas and at the surface, respectively.

$$(C_b - C_s) = \frac{r_{obs}}{k_m a_m} = 1.97 \times 10^{-8} \text{ mol/m}^3$$

Consider the difference of the bulk and surface concentration is small. It means that the external mass transport has no effect on the phthalic anhydride oxidation reaction rate.

2. Internal diffusion limitation

Next, consider the internal diffusion limitation of the phthalic anhydride reaction. An effectiveness factor, η, was defined in order to express the rate of reaction for the whole catalyst pellet, r_p, in terms of the temperature and concentrations existing at the outer surface as follows:

$$\eta = \frac{\text{actual rate of whole pellet}}{\text{rate evaluated at outer surface conditions}} = \frac{r_p}{r_s}$$

The equation for the local rate (per unit mass of catalyst) may be expected functionally as r = f(C,T).

Where C represents, symbolically, the concentrations of all the involved components

Then, $r_p = \eta r_s = \eta f(C_s,T_s)$

Suppose that the phthalic anhydride oxidation is an irreversible reaction A→B and first order reaction, so that for isothermal conditions $r = f(C_A) = k_1C_A$. Then $r_p = \eta k_1(C_A)_s$.

For a spherical pellet, a mass balance over the spherical-shell volume of thickness Δr. At steady state the rate of diffusion into the element less the rate of diffusion out will equal the rate of disappearance of reactant with in the element. This rate will be $\rho_p k_1 C_A$ per unit volume, where ρ_p is the density of the pellet. Hence, the balance may be written, omitting subscript A on C,

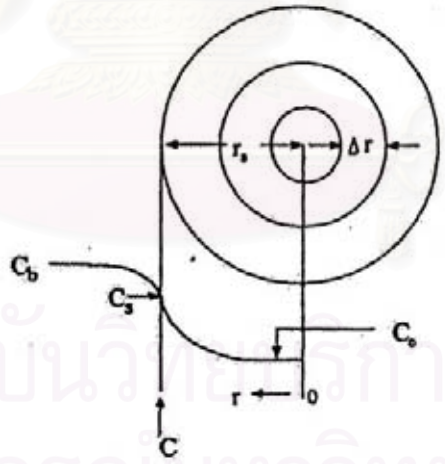

Figure B1. Reactant (A) concentration vs. position for first-order reaction on a spherical catalyst pellet.

$$\left(-4\pi r^2 D_e \frac{dC}{dr}\right)_r - \left(-4\pi r^2 D_e \frac{dC}{dr}\right)_{r+\Delta r} = -4\pi r^2 \Delta r_p k_1 C$$

Take the limit as $\Delta r \to 0$ and assume that the effective diffusivity is independent of the concentration of reactant, this difference equation becomes

$$\frac{d^2C}{dr^2} + 2\frac{dC}{dr} - \frac{k_1\rho_p C}{D_e} = 0$$

At the center of the pellet symmetry requires

$$\frac{dC}{dr} = 0 \text{ at } r = 0$$

and at outer surface

$C = C_s$ at $r = r_s$

Solve linear differential equation by conventional methods to yield

$$\frac{C}{C_s} = \frac{r_s \sinh\left(3\phi_s \frac{r}{r_s}\right)}{r \sinh 3\phi_s}$$

where ϕ_s is Thiele modulus for a spherical pellet defined by $\phi_s = \frac{r_s}{3}\sqrt{\frac{k_1\rho_p}{D_e}}$

Both D_e and k_1 are necessary to use $r_p = \eta k_1 (C_A)_s$. D_e could be obtained from the reduced pore volume equation in case of no tortuosity factor.

$$D_e = (\varepsilon_s^2 D_{AB})$$

$$D_e = (0.5)^2 (1.123) = 0.281$$

Substitute radius of catalyst pellet, $r_s = 7.6\times10^{-5}$ m with ϕ_s equation

$$\phi_s = 9.253\times10^{-7}\sqrt{k} \text{ (dimensionless)}$$

Find k (at 500°C) from the mass balance equation around plug-flow reactor.

$$r_w = \frac{F_{Ao}\, dx}{dW}$$

where $r_w = kC_A$

Thus, $$kC_A = \frac{F_{Ao}\, dx}{dW}$$

$$kC_{Ao}(1-x) = \frac{F_{Ao}\, dx}{dW}$$

$$W = \frac{F_{Ao}}{kC_{Ao}} \int_0^{0.998} \frac{1}{1 - x}\, dx$$

$$k = 0.262\ m^3/s\text{-}kg\ catalyst$$

Calculate ϕ_s : $\phi_s = 9.253\times10^{-7}\ \sqrt{0.262}$

$= 4.74\times10^{-7}$

For such small values of ϕ_s it was concluded that the internal mass transport has no effect on the rate of phthalic anhydeide oxidation reaction.

APPENDIX C

CALCULATION OF SPECIFIC SURFACE AREA

From Brunauer-Emmett-Teller (BET) equation [Anderson and co-worker (1985)]

$$\frac{p}{n(1-p)} = \frac{1}{n_m C} + \frac{(C-1)p}{n_m C} \qquad (C1)$$

Where, p = Relative partial pressure of adsorbed gas, P/P_0

P_0 = Saturated vapor pressure of adsorbed gas in the condensed state at the experimental temperature, atm

P = Equilibrium vapor pressure of adsorbed gas, atm

n = Gas adsorbed at pressure P, ml. at the NTP/g of sample

n_m = Gas adsorbed at monolayer, ml. at the NTP/g of sample

C = $\text{Exp}\,[(H_C - H_l)/RT]$

H_C = Heat of condensation of adsorbed gas on all other layers

H_l = Heat of adsorption into the first layer

For the single point method, the graph must pass through the origin. Therefore, the value of C must be assumed to be infinity.

$C \rightarrow \infty$, then equation C1 is reduced to

$$\frac{p}{n(1-p)} = \frac{p}{n_m}$$

$$n_m = n(1 - p) \qquad (C2)$$

The surface area, S, of the catalyst is given by

$$S = S_b \times n_m \qquad (C3)$$

From the gas law

$$\frac{P_b V}{T_b} = \frac{P_t V}{T_t} \qquad (C4)$$

Where, P_b = Pressure at 0°C

P_t = Pressure at t°C

T_b = Temperature at 0°C = 273.15 K

T_t = Temperature at t°C = 273.15 + t K

V = Constant volume

Then, $P_b = (273.15/ T_t) \times P_t = 1$ atm

Partial pressure

$$P = \frac{[\text{Flow of } (He + N_2) - \text{Flow of } He]}{\text{Flow of } (He + N_2)} \quad \text{(C5)}$$

= 0.3 atm

For nitrogen gas, the saturated vapor pressure equals to

P_0 = 1.1 atm

then, $p = P/P_0 = 0.3/1.1 = 0.2727$

To measure the volume of nitrogen adsorbed, n

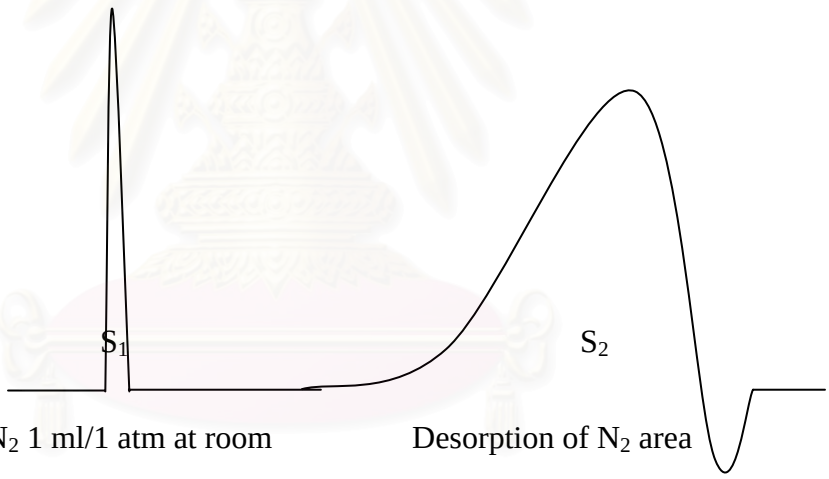

N_2 1 ml/1 atm at room temperature area

Desorption of N_2 area

$$n = \frac{S_2}{S_1} \times \frac{1}{W} \times \frac{273.15}{T} \text{ ml/g of catalyst} \quad \text{(C6)}$$

Where, S_1 = N_2 1 ml/1 atm at room temperature area

S_2 = Desorption of N_2 area

W = Sample weight, g

T = Room temperature, K

Therefore,

$$n_m = \frac{S_2}{S_1} \times \frac{1}{W} \times \frac{273.15}{T} \times (1 - p)$$

$$n_m = \frac{S_2}{S_1} \times \frac{1}{W} \times \frac{273.15}{T} \times 0.7272 \qquad \text{(C2.1)}$$

Whereas, the surface area of nitrogen gas from literature equal to

S_b = 4.373 m^2/ml of nitrogen gas

Then,

$$S = \frac{S_2}{S_1} \times \frac{1}{W} \times \frac{273.15}{T} \times 0.7272 \times 4.343$$

$$S = \frac{S_2}{S_1} \times \frac{1}{W} \times \frac{273.15}{T} \times 3.1582 \ m^2/g \qquad \text{(C7)}$$

APPENDIX D

CALIBRATION CURVE

Flame ionization detector gas chromatographs Shimadzu model 9A equipped with a Chromosorb WAW column is used to analyze the concentrations of phthalic anhydride, maleic anhydride, acetic acid, ethylbenzene, toluene, hexane and benzene.

The Porapak-Q and Molecular Sieve 5-A column are used with a gas chromatograph equipped with a thermal conductivity detector, Shimadzu model 8A, to analyze the concentration of CO_2 and CO.

The calibration curves of phthalic anhydride, hexane and carbon dioxide are illustrated in the following figures.

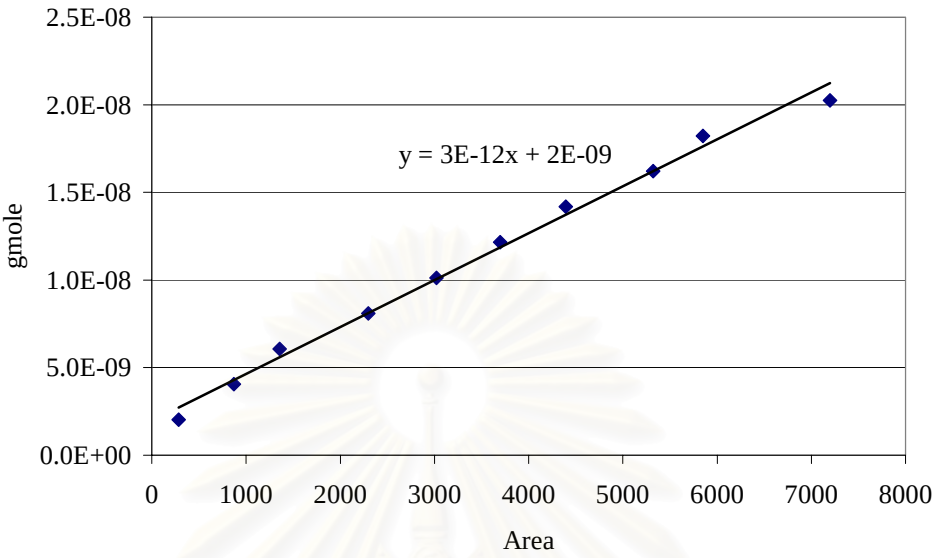

Figure D1 The calibration curve of phthalic anhydride

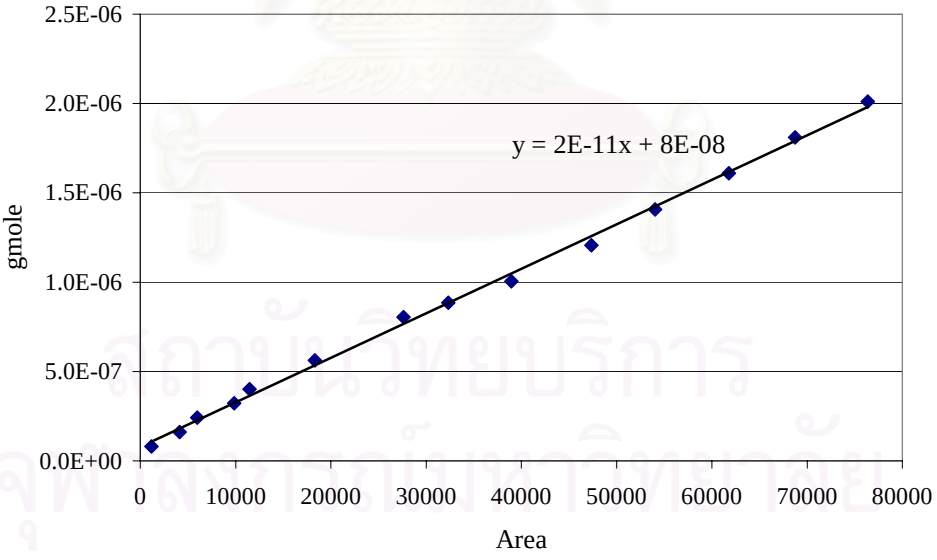

Figure D2 The calibration curve of carbon dioxide

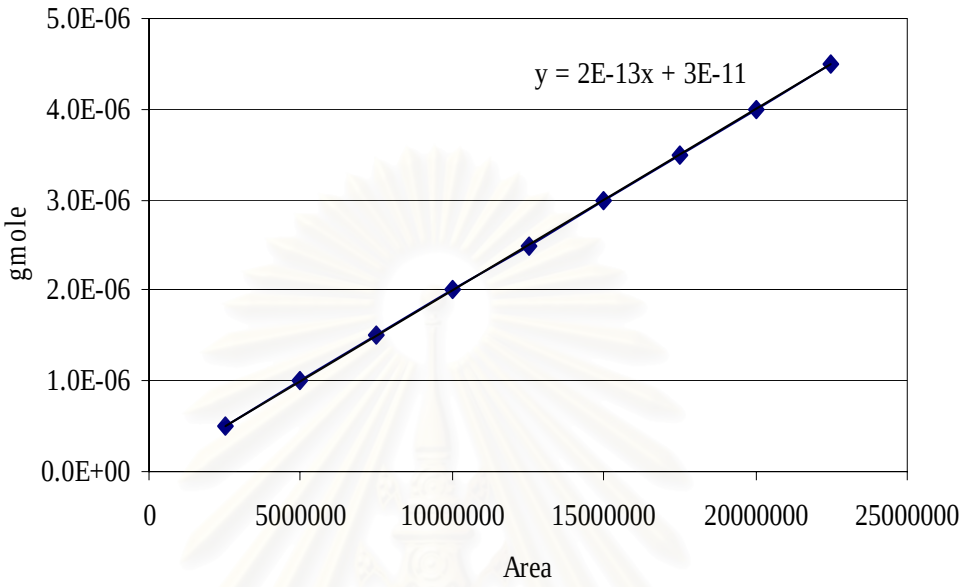

Figure D2 The calibration curve of Hexane

APPENDIX E

DATA OF EXPERIMENTS

Table E1 Data of Figure 5.2 and Figure 5.3

Temp (°C)	Phthalic anhydride conversion (%)	
	8Cu-7V-1Mg-O/ TiO_2	8Fe-7V-1Mg-O/ TiO_2
200	3.00	2.70
250	33.00	16.50
280	60.00	37.00
300	76.00	55.00
350	81.00	73.00
400	83.00	82.00
450	89.00	91.00
500	95.00	93.00

Table E2 Data of Figure 5.4 and Figure 5.5

Temp (°C)	Phthalic anhydride conversion (%)	
	8MO-7V-1Mg-O/ TiO_2	8Zn-7V-1Mg-O/ TiO_2
200	8.00	5.00
250	16.50	54.00
280	35.00	62.00
300	45.00	69.00
350	63.00	73.00
400	78.00	80.00
450	89.00	90.00
500	93.50	90.00

Table E3 Data of Figure 5.6 and Figure 5.7

Temp (°C)	Hexane conversion (%)	
	8Cu-7V-1Mg-O/ TiO_2	8Fe-7V-1Mg-O/ TiO_2
200	8.14	2.00
250	10.35	3.78
280	31.51	10.05
300	75.21	52.03
350	82.03	59.34
400	90.51	60.87
450	94.45	73.22
500	97.53	83.89

Table E4 Data of Figure 5.8 and Figure 5.9

Temp (°C)	Hexane conversion (%)	
	8MO-7V-1Mg-O/ TiO_2	**8Zn-7V-1Mg-O/ TiO_2**
200	5.82	4.89
250	11.91	3.78
280	15.95	10.05
300	59.93	43.99
350	69.56	61.88
400	74.23	62.06
450	80.62	74.37
500	86.17	85.51

Mixture

Table E5 Data of Figure 5.11 and Figure 5.11

Temp (°C)	8Cu-7V-1Mg-O/ TiO_2	
	Hexane conversion (%)	**PA conversion (%)**
200	1.18	5.60
250	2.56	31.00
280	56.00	66.00
300	64.00	73.00
350	74.00	79.00
400	81.00	81.00
450	88.00	82.50
500	95.00	84.00

Table E6 Data of Figure 5.12 and Figure 5.13

Temp (°C)	8Fe-7V-1Mg-O/ TiO_2	
	Hexane conversion (%)	**PA conversion (%)**
200	7.23	2.21
250	6.41	27.13
280	39.51	42.74
300	58.91	62.36
350	70.31	80.78
400	73.97	80.96
450	80.06	81.44
500	87.12	83.48

Table E7 Data of Figure 5.14 and Figure 5.15

Temp (°C)	8Mo-7V-1Mg-O/ TiO_2	
	Hexane conversion (%)	**PA conversion (%)**
200	3.87	5.24
250	14.80	8.60
280	44.88	39.16
300	58.39	52.11
350	61.55	59.23
400	67.95	67.95
450	77.79	73.74
500	81.70	79.50

Table E8 Data of Figure 5.16 and Figure 5.17

Temp (°C)	8Zn-7V-1Mg-O/ TiO_2	
	Hexane conversion (%)	**PA conversion (%)**
200	4.86	6.67
250	4.43	34.49
280	16.50	49.18
300	49.88	53.55
350	57.95	70.36
400	63.22	79.28
450	65.12	84.46
500	71.68	85.30

Table E9 Data of pyridine and maleic anhydride adsorption of Table 5.3

Metal	**Pyridine adsorption**	**Maleic anhydride adsorption**
8Cu-7V-1Mg-O/ TiO_2	2566777	1675645
8Fe-7V-1Mg-O/ TiO_2	3114910	1823418
8Mo-7V-1Mg-O/ TiO_2	5824161	2761236
8Zn-7V-1Mg-O/ TiO_2	4185471	1371055

APPENDIX F

MATERIAL SAFETY DATA SHEETS

Phthalic anhydride

Safety data for phthalic anhydride

General

Synonyms: 1,2-benzenedicarboxylic acid anhydride, phthalic acid anhydride

Molecular formula: $C_8H_4O_3$

Physical data

Appearance: white crystalline solid with choking odor

Melting point: 131°C

Boiling point: 295°C

Vapour density: 5.1 (air=1)

Density (g cm^{-1}): 1.53

Flash point: 152°C (closed cup)

Explosion limit: 1.7-10.5%

Water solubility: slight

Stability

Stable. Combustible. Incompatible with strong oxidizing agents, strong bases, moisture, nitric acid, alkalies. Dust may form an explosive mixture with air.

Toxicology

Corrosive - causes burns. Harmful if swallowed or inhaled. Skin or eye contact may cause severe irritation. Typical TLV/TWA 1 ppm. Typical STEL 4 ppm. Typical PEL 2 ppm.

Personal protection

Safety glasses, gloves, adequate ventilation.

Hexane

Safety data for Hexane

General

Synonyms: n-hexane, normal hexane

Molecular formula: C_6H_{14}

Physical data

Appearance: colourless liquid

Melting point: -95 C

Boiling point: 69 C

Vapour density: 3 (air = 1)

Vapour pressure: 132 mm Hg at 20 C

Specific gravity: 0.659

Flash point: -10 F

Explosion limits: 1.2% - 7.7%

Autoignition temperature: 453 F

Stability

Stable. Incompatible with oxidising agents, chlorine, fluorine, magnesium perchlorate. Highly flammable. Readily forms explosive mixtures with air. Note low flash point.

Toxicology

May cause impaired fertility. Harmful by inhalation, ingestion or skin absorption. Irritant. May cause CNS depression. Prolonged exposure may cause serious health damage.

Personal protection

Safety glasses. Effective ventilation.

APPENDIX G
PROCEDURE AND CALCULATION OF PYRIDINE AND MALEIC ANHYDRIDE ADSORPTION

Pyridine Adsorption

The nitrogen gas flowed through the system that consisted of a tube connected to the gas chromatograph (GC9A). The sample was placed in the tube as shown in Figure G1.

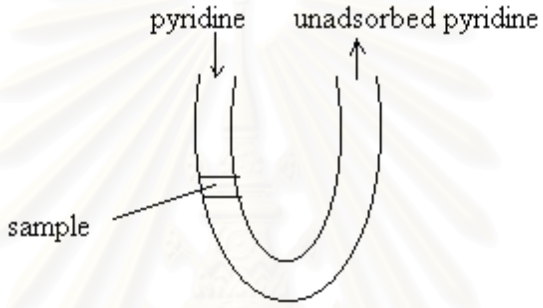

Figure G1 The adsorption system

The pyridine was injected into the column. The sample would adsorb a part of the pyridine. The pyridine that was not adsorbed on the sample was measured by the gas chromatograph. The pyridine was injected until the peaks were constant. It meant that the sample was saturated with pyridine.

The peaks of the unadsorbed pyridine that were detected from the gas chromatograph were shown in Figure G2.

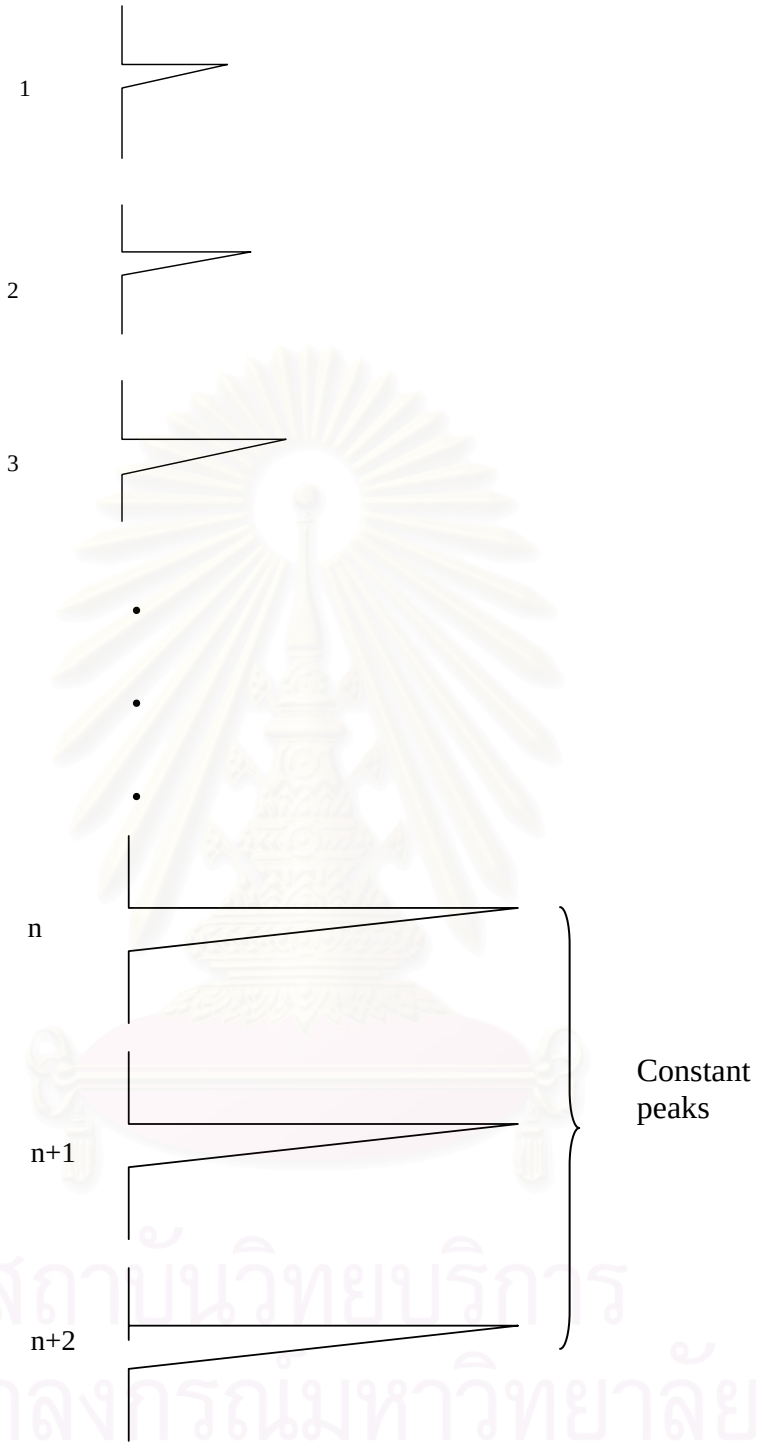

Figure G2 The unadsorbed pyridine peaks

The overall pyridine adsorbed was calculated by subtraction the area of constant peaks with the 1st peak, 2nd peak, …, respectively. The summation of these subtracted areas was the overall area of the pyridine adsorbed.

Overall pyridine adsorbed = $\sum$ (area of constant peak – area of $peak_i$)

Maleic anhydride adsorption

The procedure of the maleic anhydride adsorption was the same as the procedure of the pyridine adsorption but the pyridine injection was changed to the maleic anhydride injection. An aqueous solution of maleic anhydride (0.104 g/ml) was used.

APPENDIX H

FT-IR

Figure H-1 showed the IR spectra obtained from adsorbed pyridine on the catalysts at room temperature. It is cleared from the present work and other published works that the spectrum of the adsorbed pyridine at the room temperature shows the band at 1445 cm^{-1} and the band near 1600 cm^{-1} due to coordinative adsorbed pyridine on Lewis acid sites. The weaker band around 1480 cm^{-1} is ascribed to proton acidity [Parry (1973)], while both band at 1540 cm^{-1} and 1640 cm^{-1} representative of pyridium ions adsorbed on Brönsted acid sites which are not observe in this experiment. The IR spectra obtained from the adsorbed pyridine on the catalysts at 100°C up to 500 °C not found any significant.

-for 8Mo1Mg7V/TiO_2 catalyst cannot measure FT-IR pyridine adsorption because no peak appear after dope pyridine. But pyridine adsorption measure by gas chromatograph. can detect amount of pyridine adsorption of 8Mo1Mg7V/TiO_2 catalyst. The different of two techniques was pressure so pyridine may not adsorb on 8Mo1Mg7V/TiO_2 catalyst at very low pressure (vacuum).

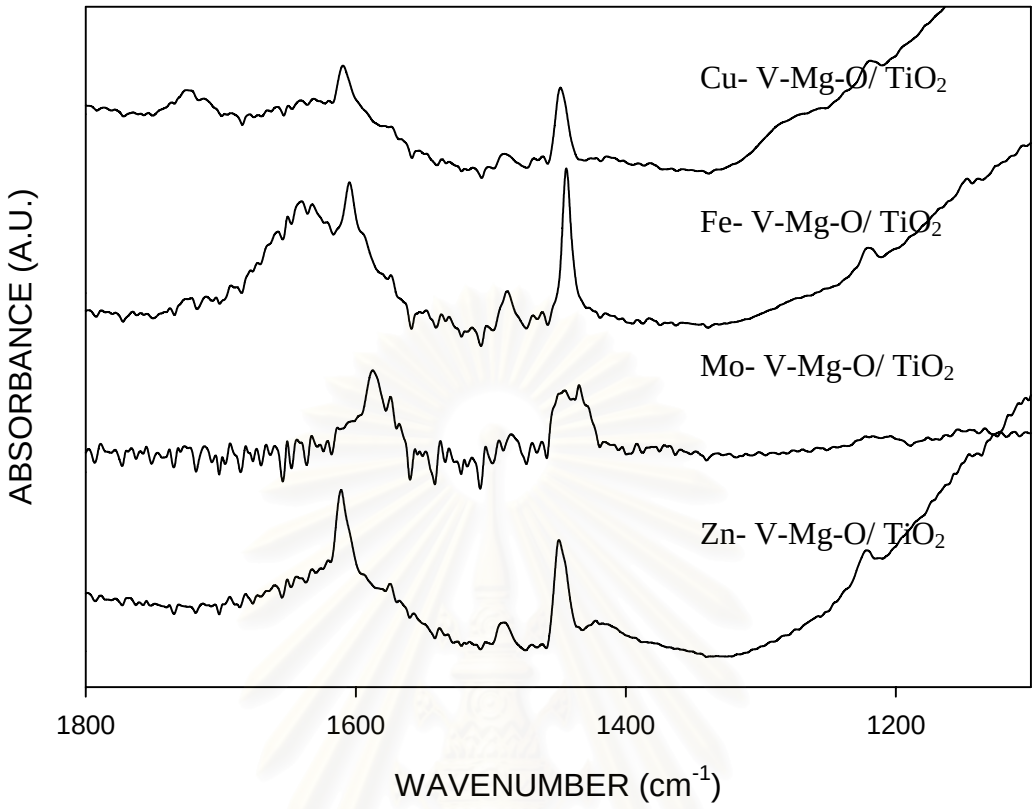

Figure H-1 Pyridine adsorption on the catalysts at room temperature

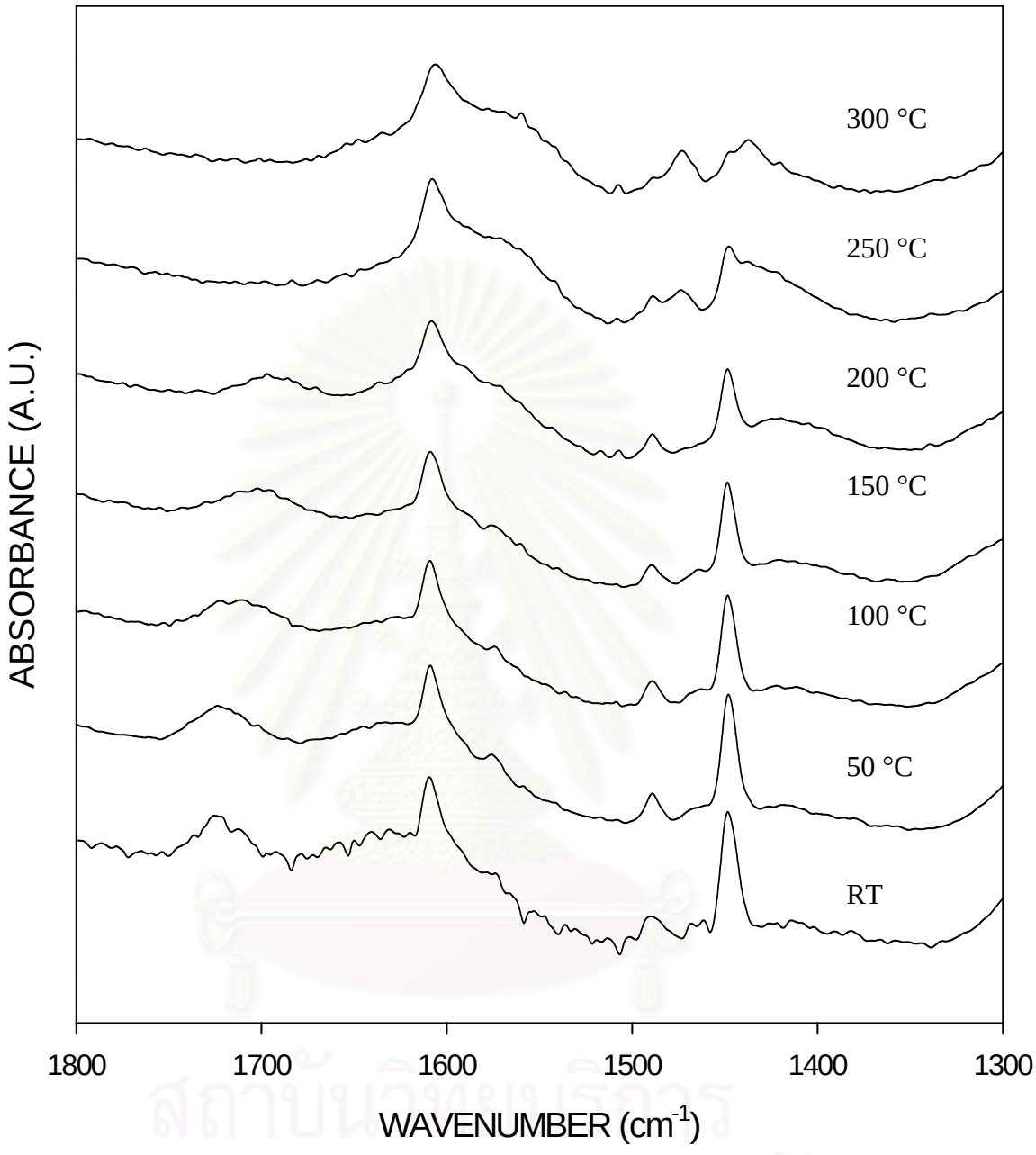

Figure H-2 Pyridine adsorption on the 8Cu7V1Mg/TiO_2 catalyst

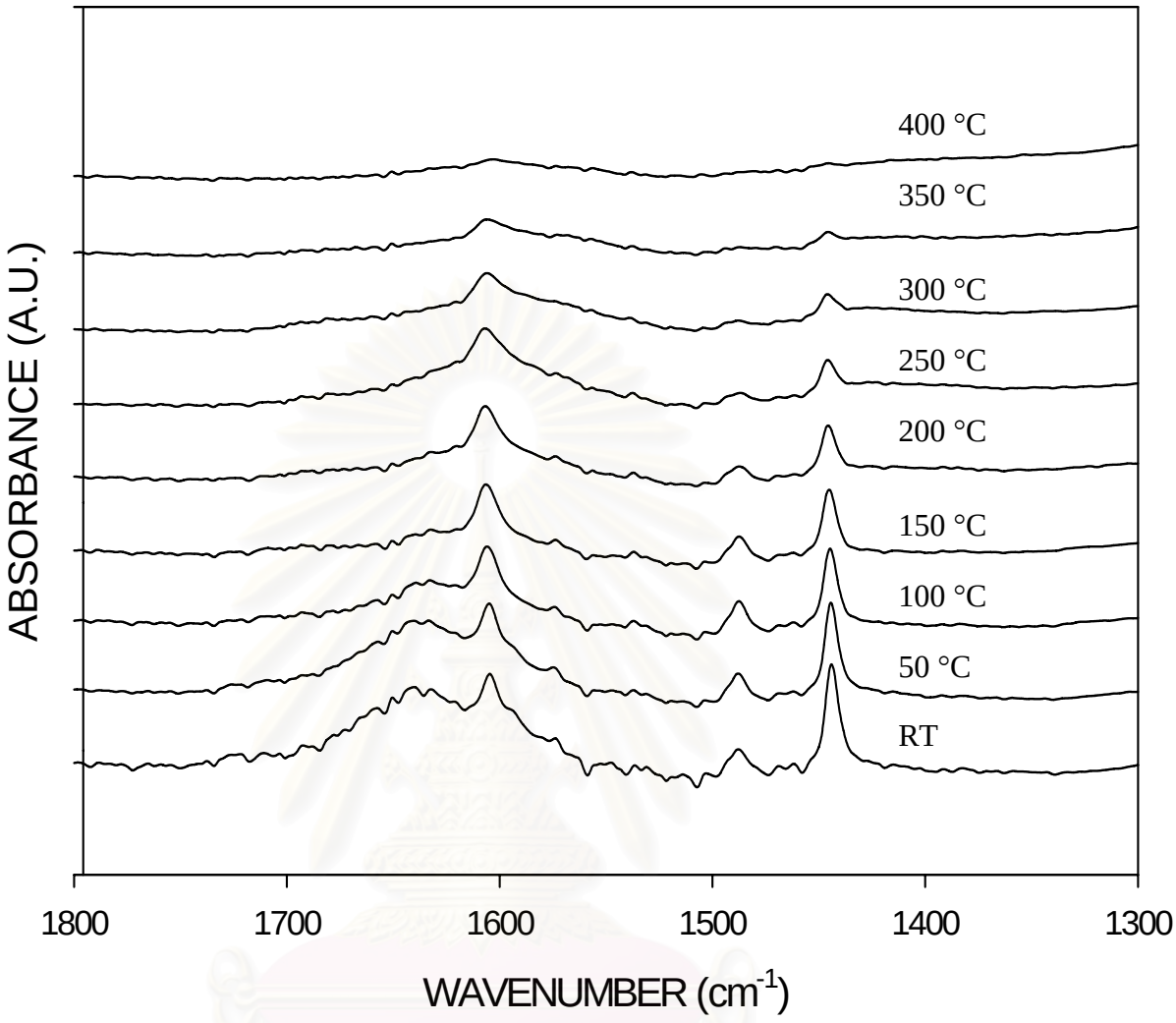

Figure H-3 Pyridine adsorption on the 8Fe7V1Mg/TiO_2 catalyst

-for 8Fe1Mg7V/TiO_2 catalyst found the band at 1644 cm^{-1} which disappeared after pretreatment under vacuum at 150 °C. It believed that this band can be assigned to OH deformation (adsorbed water on catalyst surface) [Hayes N.W. (1996)].

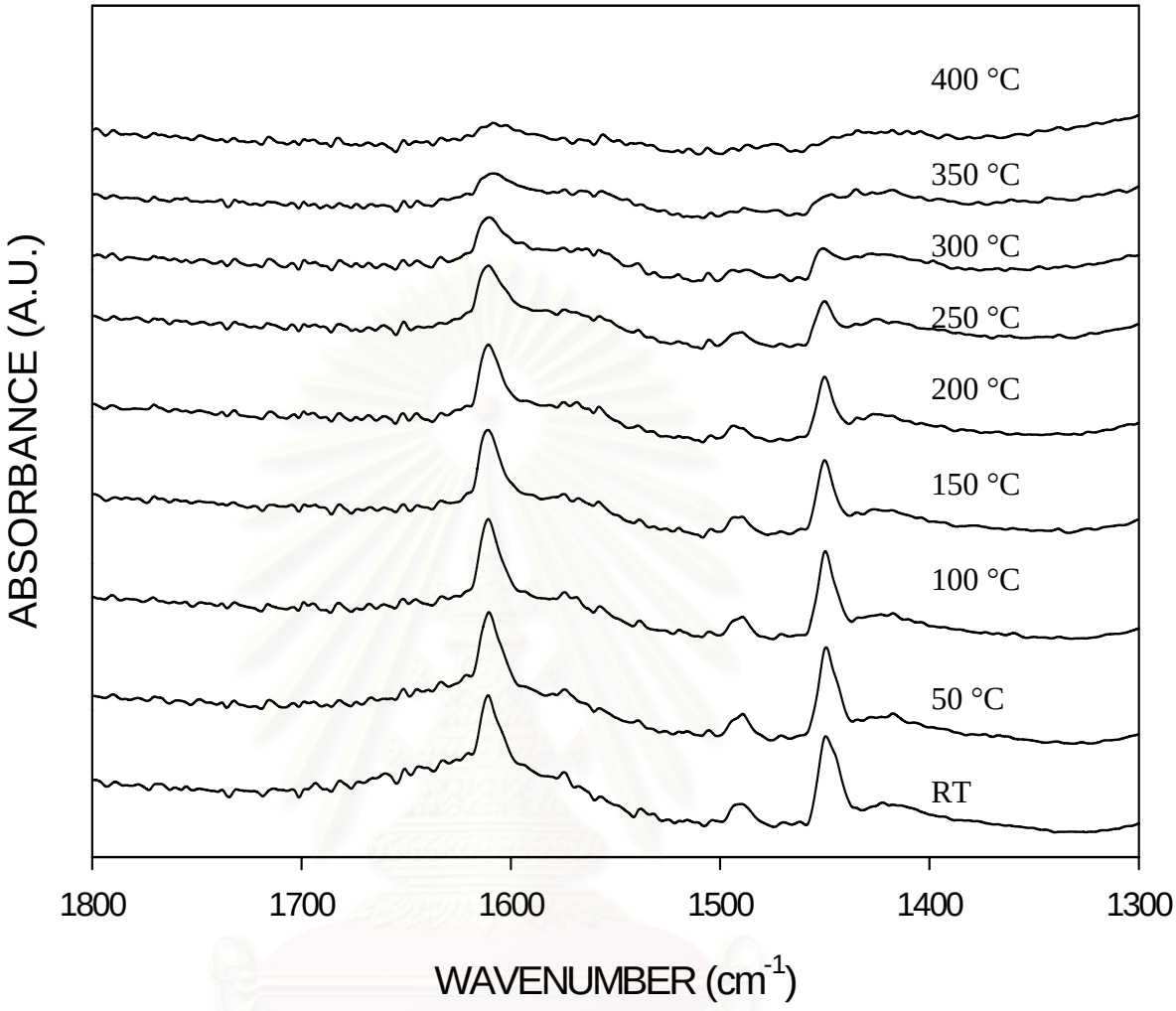

Figure H-4 Pyridine adsorption on the 8Zn7V1Mg/TiO_2 catalyst

VITA

Mr. Surakit Punjasamud was born on December 18th, 1980 in Bangkok, Thailand. He received the Bachelor Degree of Chemical Engineering from Faculty of Engineering, Kasetsart University in 2002. He continued his Master's Study at Chulalongkorn University in June, 2003.